THE UNIVERSITY OF WESTERN ONTARIO
DEPARTMENT OF CIVIL AND
ENVIRONMENTAL ENGINEERING

Water Resources Research Report

Development of Inundation Maps for the Vancouver Coastline Incorporating Effects of Sea Level Rise and Extreme Events

By:

Nick Agam
and
Slobodan P. Simonovic

Development of Inundation Maps for the Vancouver Coastline Incorporating the Effects of Sea Level Rise and Extreme Events

By

Nick Agam

and

Slobodan P. Simonovic

Department of Civil and Environmental Engineering

The University of Western Ontario

London, Ontario, Canada

March 2015

Table of Contents

List of Tables

List of Figures

Executive Summary

The increased greenhouse gases in the atmosphere is heating up the world, resulting in global warming. The effects of this are many, this study is focused on the effects of Sea Level Rise (SLR) and what it will do to coastal communities.

Sea level rise (SLR) is a hazard that has the potential to redefine the world's coastlines. The effects of SLR can lead to more severe storm surges, flooding and inundation causing disasters for coastline populations and environments. There are two main concerns that are attached to SLR, the steady rise in the global mean sea level (GMSL) and the increase in frequency and magnitude of all wave events. The effects of SLR in both cases are increased risk of flooding, damage to infrastructure, erosion and damage to natural eco systems. These concerns effect all those who live on the coast where the worst case situation is permanent inundation of land. This change is caused by a number of factors - thermal expansions, inputs from glaciers, ice caps and ice sheets and changes in land water storage. To help mitigate the effects of SLR, the areas at risk should be identified. The most common way to understand the effects of SLR and their potential dangers is to visualize the impacts using the inundation maps. The goal of the research presented in this study is to (a) develop the methodology for mapping the impacts of SLR and (b) create inundation maps for the Vancouver coastline for the next 100 years.

In this study a methodology is created to develop inundation maps for the Vancouver coastline (British Columbia, Canada) with the use of public data and GIS software. The rates of SLR used are linear rates developed by the Intergovernmental Panel on Climate Changes (IPCC) which incorporate the effects of climate change. Two methods are discussed, a deterministic method and a probabilistic method. The deterministic method adjusts the IPCCs rates to consider the regional tidal patterns and vertical land movements and for Vancouver to determine sea level elevation values. The probabilistic method considers extreme events, and utilizes cumulative distribution functions (CDFs) to determine sea level elevation values. A factor is used to incorporate the effects of SLR into the CDFs. Using the two methods as inputs for sea level elevation values a SLR simulation process was created using GIS software. The end result of the process is inundation maps for the Vancouver coastline that incorporate the effects of SLR and extreme events.

1. Introduction

1.1 Climate Change and Sea Level Rise

The influence of climate change is an important consideration in the coming decades. The world has become interested in how the changing climate could affect the future. To gain a better understanding of the effects of climate change, models are created to simulate potential future scenarios. Numerical models referred to as General Circulation Models (GCMs), are created with the goal of predicting the future climate. The creations of these models are based on many assumptions. Each model makes different assumptions, and it is the difference in these assumptions that results in variability amongst models. Because of the different assumptions a single model can produce multiple scenarios. The outcomes of the scenarios vary to incorporate a realistic best and worst case situations of how the future may unfold. The goal of these projections and scenarios are to gain a better understanding of the effects of climate change with hopes of mitigation.

One main impact of climate change is Sea Level Rise (SLR). Within the past 100 years the rate of SLR has accelerated (The COMET Program, 2012). This acceleration is causing coastal environments to shift away from their predictable state to a new one. With the help of climate models, scenarios have been developed to gain a better idea of the degree of SLR for the next 100 years.

Given the time scale of the projections SLR is a long term problem that must be planned for in the coming years. Any future development must be aware of this problem and consider the effects during the planning and design stage. To properly consider the effects of SLR all projections must be known and analyzed. Using this knowledge the most realistic projection values must be used for future development. Even though there is a large amount of uncertainty attached to SLR costal communities must be aware and plan accordingly.

1.2 Objective of the Study

The main objective of this report is to develop inundation maps for the area of British Columbia, Canada. Using regional constructed rates inundation maps are created to depict areas of inundation caused by SLR. Global SLR rates are adjusted for the region of Vancouver by

considering regional tidal patterns and the effects of vertical land movements. Two methods were used to define the future sea level elevation, a deterministic analysis method and a probabilistic analysis method. Using these two methods inundation maps were created for the Vancouver coastline.

1.3 Research Procedure

For this report the two methods for determining sea level elevation will be discussed. The deterministic method utilizes the IPCCs global SLR rates and factors in regional considerations. The method considers the natural movement of tides for the Vancouver region as well as vertical land movements (VLMs). The probabilistic method utilizes extreme value analysis, which is a branch of statistics that deals with the extreme values (larger or smaller than the median) from a given dataset (Coles, 2001). The benefits of using such an analysis is that the extreme events can be assigned a frequency. This analysis can be used with tidal gauge data to determine when the extreme events occur .The end goal of this method is to develop cumulative distribution functions (CDFs) of sea level elevation for extreme events for a region while considering the effects of SLR. Once sea level elevation values are found the inundation maps were created using ArcGIS (ESRI, 2011) and its integrated Python feature (Python Software Foundation, 2014).

1.4 Organization of the Report

This report is comprised of 5 sections. Section 2 of this report is used as a brief literature review. Section 3 of the report is dedicated to the methodology followed for both the deterministic method and probabilistic method as well as a discussion on the simulation process for developing inundation maps. Section 4 of the report describes the case study and applies the methodology to the area of Vancouver (British Columbia, Canada). The final section is used to conclude the report and discuss the final results.

2. Literature Review

SLR is a long term problem, which must be considered for future development. The biggest concerns are inundation of land and development of infrastructure in these affected areas. However inundation is not the only concern as a higher sea level will provide a higher base for storm surges to build on, thus increasing the risk of flooding, infrastructure damage, erosion and damage to natural eco systems.

The main concern when planning for the effects of SLR is the uncertainty associated with the SLR predictions. Typically town planning is done assuming a constant sea level. It is essential to change this and conduct planning with a dynamic coastline (The Arlington Group Planning and Architecture Inc. et al 2013). High level of uncertainty related to the future GMSL is making planning hard (Sahin and Mohamed 2010). Therefore the best plan is to define the areas of inundation for a range of SLR impacts by considering the best and worst case scenarios the future of coastal communities will face.

Predicting sea level rise rates for future dates can be based on a detailed analysis of historic trends. When looking at the historic trends there are two types of data available, tidal gauge and satellite-based radar altimeter data. Using tidal gauge data from 1901-2010 the long term trend estimate in GMSL is 1.7mm/year. This results in a total sea level rise of .19m since 1901. Satellite altimeter records only date back to 1992 (Church et al, 2013). The satellites are used to provide nearly global sea-level measurements at 10-day intervals. Using this data a GMSL rate of 3.2mm/year is estimated for the years for 1993-2012 (Church et al, 2013). Comparing the two data sources leaves one to conclude that the rate of SLR is accelerating. The source of this acceleration is still in question, as multi-decadal variations play a large role in varying the rate of SLR on a larger time scale. The IPCC have determined that in terms of future SLR rates it is 66–100% certain that these rates will only increase in the coming years. It is expected that the rate of SLR is going to increase even after greenhouse gases (GHGs) are stabilized (Church et al, 2013; PostNote 363, 2010).

The biggest uncertainty attached to SLR is determining the actual rate of SLR. Considering the number of contributing factors and their surrounding uncertainty, finalizing a rate of SLR is very difficult. In 2013 the Intergovernmental Panel on Climate Change (IPCC) came out with their fifth assessment report, the AR5 (Church et al, 2013). This report covers a wide range of

problems that are related to the changing climate. Chapter 13 of the report is dedicated to sea level change, and is used to discuss the different input factors, areas of uncertainty and also rates of sea level rise. The AR5 (Church et al, 2013) was used to introduce four new scenarios.

The four scenarios are known as the following (Church et al, 2013) :

1. RCP 2.6
2. RCP 4.5
3. RCP 6.0
4. RCP 8.5

The scenarios are named according to their 2100 radiative forcing level and are four different and independent pathways, developed by four different research groups. There is no link between the scenarios, meaning that the higher radiative forcing scenarios are not used to derive the lower scenarios. All scenarios were created with different assumptions. Therefore the differences are not only related to the different levels of radiative forcing but also to the different assumptions used in the development of a scenario.

Figure 1 illustrates the different scenarios and their pathway shapes.
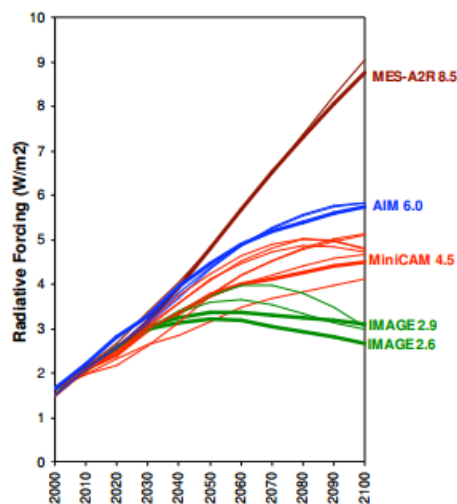
Figure 1 Four RCP scenarios

In this report, all four RCP scenarios are considered to help understand the range of possible SLR impacts. However the main focus remains on the lower and upper bound projections in order to improve the understanding of the uncertainties associated with various future projections and provide better support for decision making. Therefore the main emphasis of this study is on RCP scenarios 2.6 and 8.5.

Selection of the "most realistic" scenario is a very difficult task because of the uncertainty associated with all future projections. Decision makers must consider all projections and select one they think will be the most appropriate for problem under consideration.

The IPCC defines rates of SLR using different modeling tools. These models are process based and the processes considered by the IPCC are as follows (Church et al, 2013):

- Thermal Expansion
- Glaciers melting
- Greenland ice sheet change
- Antarctic ice sheet change
- Land water storage
- Greenland ice sheets rapid dynamics
- Antarctic ice sheet rapid dynamics

The rates of SLR are based on the results obtained from 21 CMIP5 Atmosphere–Ocean General Circulation Models (AOGCMs). The results from different models were used to create a multi-model ensemble mean which is considered to be preferable approach compared to the selection of a single model. (Church et al, 2013).

Work done by Arns et al (2013) looked at evaluating different methods of estimating probabilities of extremes. As recommended by the IPCC one strategy to deal with SLR is to protect the areas at risk. There are generally two options, advancing the line and holding the line. Both options require flood defense systems that need to be precisely designed to ensure the area will be protected over the life of the structure.

For efficient planning and design of coastal structures it is important to understand the stochastic character of extreme water level events. Design levels for coastal defense are usually defined using some form of statistical analysis (Dixon and Tawn, 1994). These analyses are

mostly based on the extreme value theory, a special subdiscipline of probability theory that deals with rare events, such as coastal floods (Coles, 2001).

Arns et al (2013) focus on two different methods of estimating CDFs. They have selected to evaluate the tidal gauge data using the block maxima method (BM) as well as the peaks over threshold method (POT).The BM method samples the dataset by selecting the largest value in each year, this is known as the r-largest value. When r=1 only one value is used per year, however to gain more insight into the dataset r can be greater than 1. For example if r=4 then the highest 4 values would be sampled. The POT method samples the data using a threshold value. A value is subjectively selected to be the threshold, any values higher than the threshold value are sampled for that year. Using both methods a methodology was developed to gain CDF graphs, using extreme value analysis. The authors look to compare both methods with the end goal of developing an objective approach for setting up the model. The methodology followed by the authors is highlighted in Figure 2.
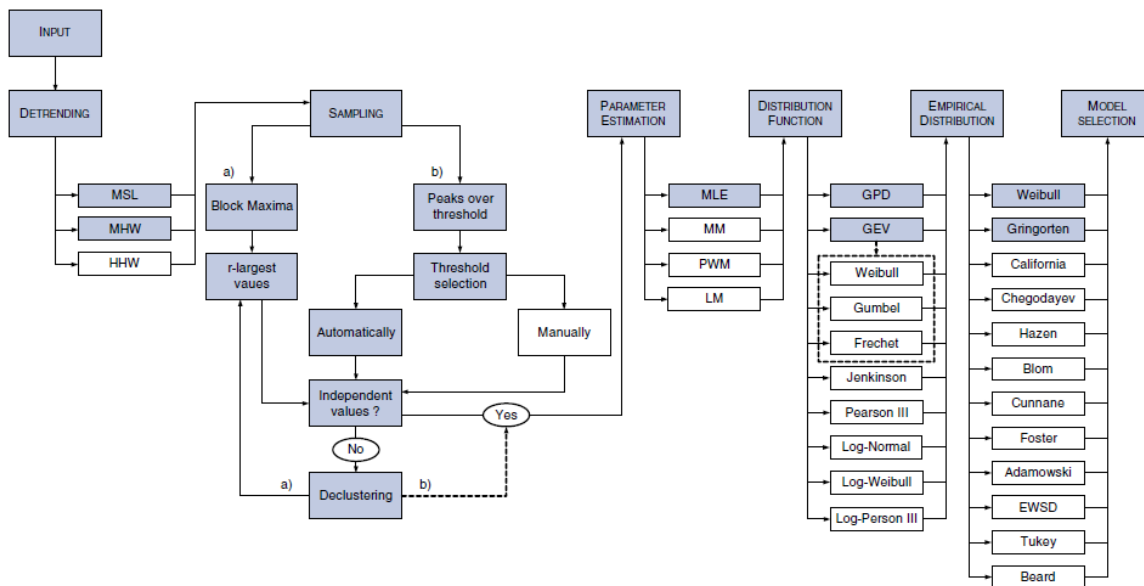
Figure 2 Methodology used by Arns et al (2013)

Input data come in the form of hourly tidal gauge data. The data is then de-trended in order to make the dataset independent and stationary. This is a fundamental assumption required for the application of statistical analysis. Arns et al, (2013) use three different methods to de-trend the

data; a linear fit covering the entire dataset, a 19-year moving average and a 1-year moving average. The trend adjusted data sets are obtained by subtracting the estimates of the trend from the original dataset. Once the datasets are de-trended, both sampling techniques are used. The BM method depends on the selected r-largest value, for sensitivity the authors use r-largest values ranging from 1-6. The POT method is dependent on the threshold value, for consistency between sampling methods the authors manage to adjust the threshold value to match the number of events in the BM derived sample. This means for a BM derived sample when r=4 the matching POT derived sample would have an adjusted threshold value so that 4 events are present.

The maximum-likelihood estimation (MLE) method is used to estimate the parameters for both BM and POT methods. Once the parameters are known the next step is to fit the samples with a distribution. The BM method is combined with a generalized extreme value (GEV) distribution, while the POT method used the generalized Pareto distribution (GPD). Once the sample datasets are fitted with the appropriate distribution the return period graphs can be constructed.

The BM methodology is used in this study to avoid the subjective selections of threshold values associated with the POT method.

One concern when determining CDFs is that the SLR distribution shape may change in the future. The main objective of a frequency analysis is to estimate the CDFs of a hydrometerological variable. CDF graphs are used to find out how often a given magnitude will occur. They can also be used as aids in the design and construction of coastal defense systems (Rakhecha and Singh, 2009). The rise of local GMSLs will cause events to occur at a higher frequency then in the past. To address this issue Church et al (2008) suggest the increase in the frequency for a given rise of the sea level. The methodology is introduced by using tidal gauge data for Fremantle, Australia. A comparison is made using two data sets, pre-1950 data and post-1950 data in the form of CDF graphs. Figure 3 shows the comparison graph.
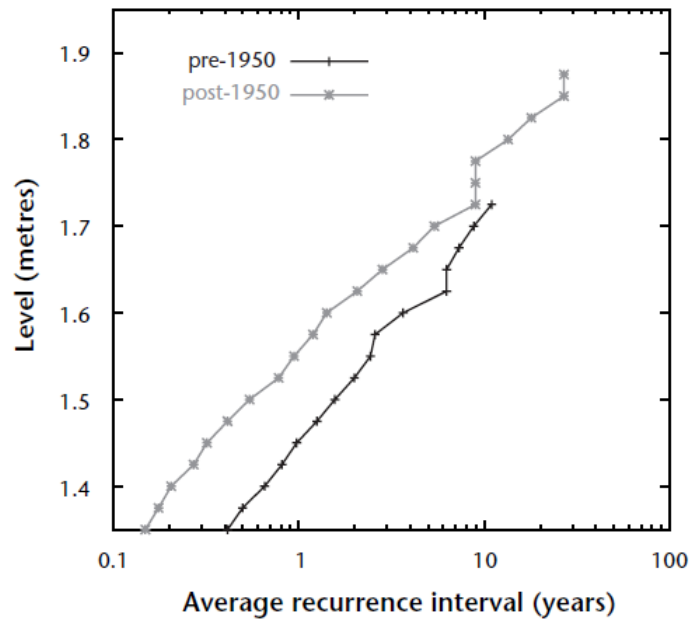
Figure 3 Pre-1950 and post-1950 CDF graph (after Church et al, 2008)

The relationship in figure 4 illustrates that the sea level varies approximately logarithmically with the average recurrence interval, indicating that the extremes approximately follow the Gumbel distribution (Church et al, 2008). The authors use the Gumbel distribution to form a factor that increases the frequency of occurrence by considering a rise in the sea level. The factor uses three variables, *r*, *h* and *H*. The sea-level rise of *h* increases the frequency of occurrence by a factor *r*, then, a future sea-level rise of *H* increases the frequency of occurrence by a factor $r^{H/h}$ (Church et al, 2008). The increase in frequency is very large, even for modest estimates of SLR.

Once projections and return periods are known the next step is to define the areas affected by the hazard using the inundation maps. The development of inundation maps can be done in a number of ways, utilizing different programs and methods. Research done by Pieper et al, (1994) developed a method to define areas of inundation using a dynamic spatial model that simulates the effects of gradual sea-level rise. The method used the dynamic properties of coastal systems in spatially explicit dynamic simulation model.

To simulate physical change in the landscape of coastal zones a base model must be created that meets the following requirements (Ruth and Pieper,1993):

1. Model must be dynamic
2. Model must represent and maintain spatial relationship of the area of study

The authors extended work by Grossmann and Eberhardt (1992) who have developed three categories of dynamic models with base maps: (i) Complex aggregate dynamic feedback models - used when system dynamics are similar over large areas; (ii) Classic transport models - , used when a process is explained with partial differential equations; and (iii) simple generic models - used when the development of each area is calculated individually . The simple generic model defines individual areas, then   includes adjacent areas and influences, and finally applies a balancing equation to calculate the alterations and update the area.

The model used by Ruth and Pieper (1993) is a cross between the classic transportation model and the simple generic model. Each area is defined using the generic model then any intercellular flows are described with the transportation model. This approach allows for three main considerations that other approaches don't have. It is very general and versatile in terms of the dynamics of the physical processes, it has a general structure and allows for inputs, and finally it considers the actual topography of the study area.

The model structure is a 25 model cell configuration with three types of cells land, water and marsh, where for each cell the average elevation was known. In this model for simplicity a given cell would be influenced by only four adjacent cells, rather than eight. Figure 4 illustrates what cells will influence the cell of interest, the cell of interest is highlighted in red, while the influential cells are highlighted in black. The blue cells are the cells around the cell of interest but not influencing the cell.

$i+1,j-1$	$i+1,j$	$i+1,j+1$
$i,j-1$	i, j	$i,j+1$
$i-1,j-1$	$i-1,j$	$i-1,j+1$
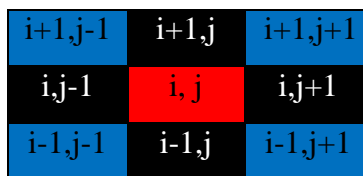
Figure 4 Cells influencing the cell of interest

A variation of this model structure is utilized in this study with an assumption that all adjacent cells have equal opportunity to influence the cell of interest. Therefore, all eight surrounding cells are used to properly simulate the effects of SLR.

The approach used by Ruth and Pieper (1993) is similar to work of Sahin and Mohamed (2010) who looked to provide a dynamic model for vulnerability assessment of coastal areas. Their model was created to simulate SLR with the consideration of three variables:

1. Cover (Land of water)
2. Elevation
3. Sea Level

However, addition of more variables adds to the complexity and uncertainty and could lead to a less accurate projections (Aral et al 2012). By simplifying the inputs to only three variables (elevation, state of adjacent cells and their proximity to water) , Aral et al (2012) produce results that are easier to interpret.

The simulation process was done by first defining the cover of a cell, whether it is land or water. Each cell is then given a specific elevation that reflects the areas natural topography. Once a cell has both a cover type and elevation value, the information is then passed to a system dynamics portion of the model. Here a reevaluation of the cover is done by comparing the elevation value to the sea level elevation. If the sea level elevation is higher than the land elevation the cover type will be converted from land to water. The specific criteria to define flooding is as follows:

1. The elevation of the cell of interest is less than the elevation of the adjacent cell

   AND

2. The adjacent cell is water

 Given these two requirements are satisfied the cell in question will be flooded and the cover type will change from land to water.

This study is using a similar methodology that to define variables and simulate flooding. The simulation process relied on a cover matrix, a land elevation matrix and a value of sea level elevation. Using these variables a comparison code was created to simulate the flooding process using the same criteria as Sahin and Mohamed (2010).

3. Methodology

To create SLR inundation maps an innovative methodology has been developed and implemented in this study. The methodology relies on two inputs: (i) land elevation in the form of DEM data, and (ii) sea level elevation that includes the effects of SLR. The sea level elevation values are obtained in the form of the inundation deterministic and a probabilistic inundation values. The purpose of using a deterministic analysis is to gain inundation maps representing the gradual rise in sea level and to map its effects. While the probabilistic analysis results in inundation maps that illustrate extreme events for the area. Figure 5 highlights the basic steps of the developed methodology.
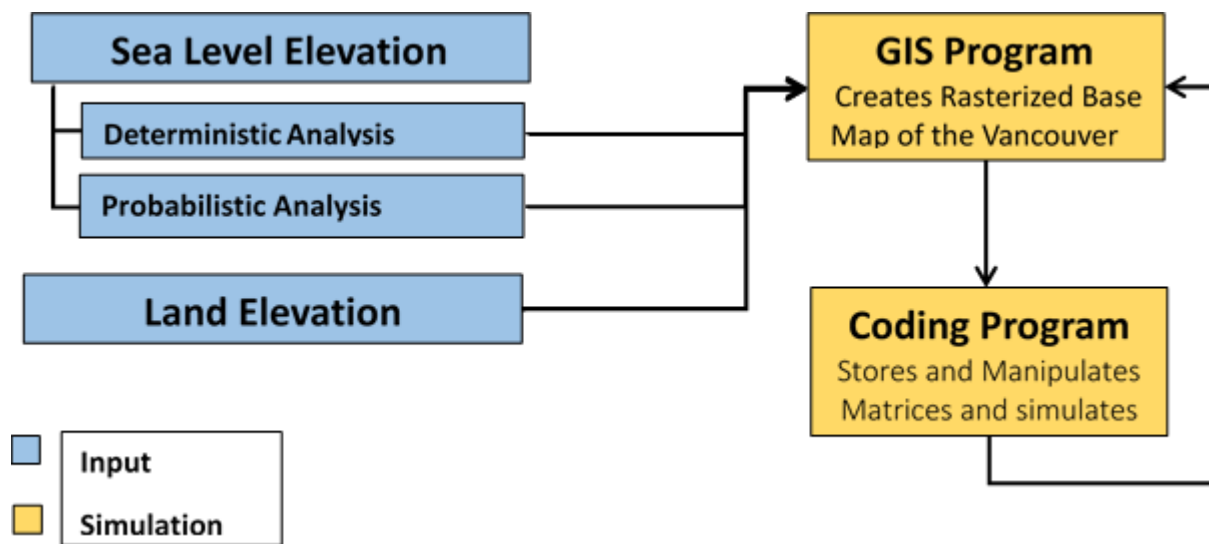
Figure 5 Basic methodology

3.1 Method 1: Deterministic Analysis

The first method utilizes the IPCCs global SLR rates and factors in regional considerations. When determining regional sea level elevation there are two main considerations that must be accounted for. The first is focused on the regions natural tidal movements. By understanding the natural tidal patterns one can begin to anticipate the magnitude of an extreme event. The natural tidal movements are forecasted using U_Tide (Codiga, D.L., 2011) which is a MATLAB (MATLAB 7.1.2, 2011) script that is used for the analysis and reconstruction of tidal gauge data. The code includes two functions, ut_solv() for analysis and ut_reconstr() for reconstruction, creating either a hindcast or forecast. The script is able to use hourly tidal gauge data as the only

input and analyze the local tidal patterns. Once the tidal patterns are forecasted the IPCCs SLR rates are added to the sea level elevation value to gain a sea level elevation that accounts for SLR.

The other regional consideration is vertical land movement (VLM). Land often experiences uplift or subsidence. In the case of uplift the land is lifting upwards at a given rate, this means that it is moving away from the mean sea level elevation. Comparing this to subsidence where the land is moving towards or below the mean sea level elevation, one can see how this plays a role when determining the rate of SLR. VLM is factored into the analysis by either subtracting the VLM value from SLR rates or adding it, corresponding to uplift or subsidence, respectively.

Once the global rates are adjusted for the region the final step is to produce equations that represent the SLR rates as a function of time. These equations are used as inputs for the simulation of SLR and the development of inundation maps.

3.2 Method 2: Probabilistic Analysis

The second method utilizes extreme value analysis, which is a branch of statistics that deals with the extreme values (larger or smaller than the median) from a given dataset (Coles, 2001). The benefits of using such an analysis is that the extreme events can be assigned a frequency. This analysis can be used with tidal gauge data because the extreme events cause the most significant damage. The end goal of this method is to develop cumulative distribution functions (CDFs) of sea level elevation for extreme events for a region while considering the effects of SLR.

The use of CDFs is very common in hydrology. The main use is to estimate the return period (t) of a variable (X) (Rakhecha and Singh, 2009). In this case the variable in question is the sea level elevation. For this method the extreme value analysis is conducted using historical high tide values which are used to predict the return period.

For this method the only input data are the hourly tidal gauge data. Using these data a process is developed to reach the end goal of CDFs of sea level that incorporate the effects of SLR. Figure 6 illustrates the methodology followed to create the CDF graphs.
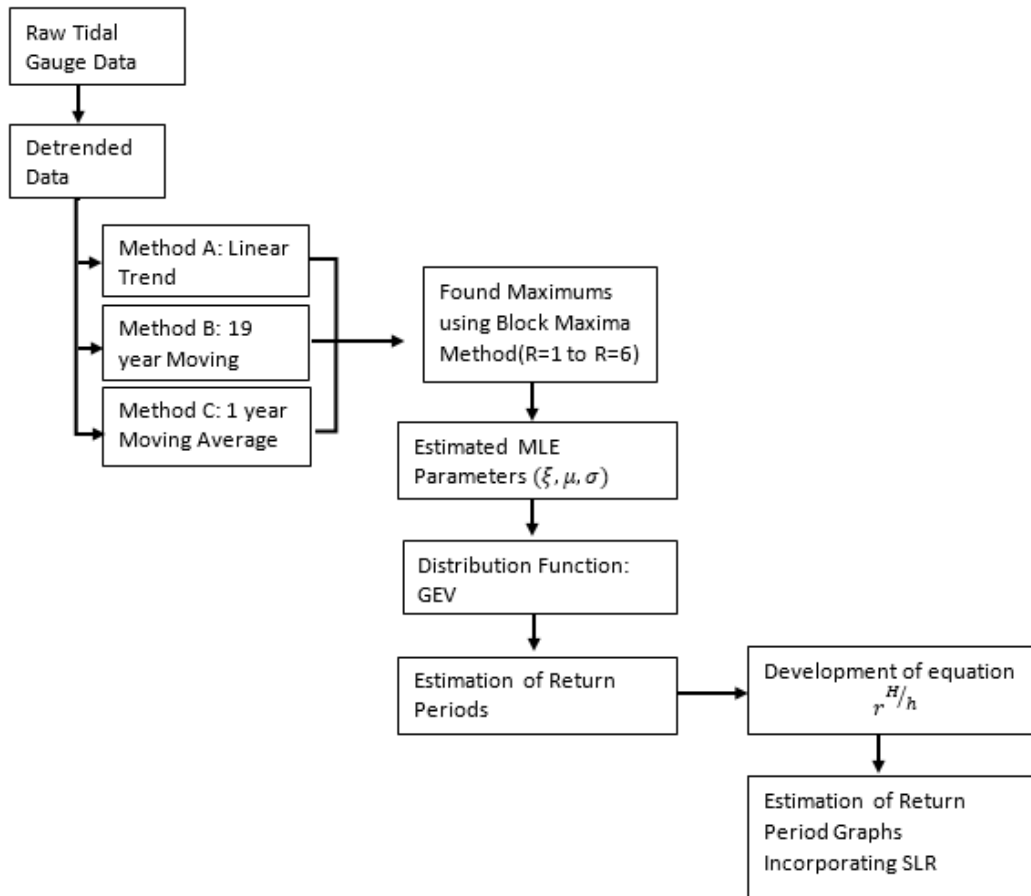
Figure 6 Flow diagram of probabilistic method for mapping SLR impacts

To keep consistency between methods hourly data was used for this analysis too. The data is detrended using three different methods. Detrending allows the data to be considered as stationary, meaning the statistical characteristics of the dataset would be held constant over time (University of Arizona, 2013). Due to the nature of the analysis detrending the data is a requirement and is done as part of data preprocessing, before a statistical analysis can take place. For this study three detrending methods are considered, where results vary depending on the selected method. The three methods being considered are: (i) a linear fit; (ii) a 19 year moving average; and (iii) a 1 year moving average. The final choice of the detrending method is

subjective and based on the results. The results leading to the worst case scenario are used as a guide for the method selection.

The sampling technique used is the BM method. In this method each year is considered as a block and each block is filtered to find the maximum values. This is known as the R-largest approach for generating BM samples (Arns et al, 2013). The blocks are further separated depending on the season (winter, spring, summer, and autumn), therefore there are 4 blocks per year.

Seasonality plays a large role, as annually some seasons are prone to have higher tides than others. This is due to meteorological, and larger atmospheric patterns. Because of this influence all data sets are split according to their season. Table 1 is a summary of the seasons and their associated months.

Table 1 Summary of seasons

Winter	Spring	Summer	Autumn
January	March	June	September
February	April	July	October
December	May	August	November

By performing an extreme value analysis on each season, annual patterns are better understood. Rather than using one value per year, one value is obtained from each season. From this set of values, the highest and lowest monthly values are used and compared, to understand the full range of possible outcomes. A subjective analysis is done to determine the maximum and minimum seasons.

To gain insight in the extreme values of the tidal records an R-largest approach is used. The number of input values is dependent on the value of R. Therefore if R=1 only one value per block is used, likewise if R=2 then the two highest values are used. For this study R values ranged from 1 to 6. It is important to consider more than 1 maximum value per block, because the maximum values in a block can vary from block to block. By considering more values a

fuller understanding of the tidal event is obtained. Another subjective analysis is done to determine an appropriate R value.

When R is greater than one, multiple events are considered. To ensure that the same event is not considered a td value is used. The td value is set to 24 hours, meaning that events must be at least 24 hours apart for them to be considered as a new event.

Once the R values (1-6) are found for each season the MLE parameters are calculated. This step is done in MATLAB (MATLAB 7.1.2, 2011) using the gevfit(x) function. This function has the following parameters for the generalized extreme value (GEV) distribution:

ξ = **Shape Parameter**

μ = **Location Parameter**

σ =**Scale Parameter**

The GEV distribution combines three types of distributions into one. It combines the Gumbel, Frechet and Weibull distributions (Coles, 2001), (Arns et al, 2013).

$$P(X \le x) = GEV = exp\left\{-\left[1 + \xi\left(\frac{Z-\mu}{\sigma}\right)\right]^{-1/\xi}\right\} \qquad 1.1$$

Equation 1.1 is used, where the Z is the detrended sea level values. This process is implemented with all three detrending methods, considering the four seasons and all R-values between 1 and 6.

Using the cumulative distribution functions (CDFs) the return periods are then calculated by the equation below (Rakhecha and Singh, 2009)

$$\frac{1}{T} = 1 - P(X \le x) \qquad 1.2$$

Once the CDFs are calculated they are plotted against the detrended sea level elevations to represent CDF graphs. This is done for all three detrending methods.

The created CDF graphs are obtained using the period for which the tidal gauge data are available. The sea level elevations are used for that the same time period. However due to SLR these events will occur more frequently and at a higher magnitude. To account for this change an equation is developed to increase both the magnitude as well as the frequency of the graphs. Incorporating SLR into the CDF graphs is done with the use of the following factor (Church et al, 2008):

$$r^{H/h}$$

Where:

$$r = the\ increase\ of\ frequency$$

$$h = historic\ sea\ level\ rise$$

$$H = future\ sea\ level\ rise$$

The factor above allows for a recalculation of the frequency given that a SLR of h increases the return period by a factor of r then, a sea level rise of H increases the frequency of an event by a factor of $r^{H/h}$ (Church *et al*, 2008).

A back transformation is required to transform the data back to the original non-detrended scale (Seltman, 2009). The purpose of detrending is to address non-stationarity due to a trend mean (University of Arizona, 2013). Now that the statistical analysis is complete the data is transformed back to the original scale. This was done by finding the time and date of the maximum values of sea level elevation and then associating it with the original value rather than the detrended one. Once the back transformation is complete the final CDF graphs can be developed.

A logarithmic extrapolation is done on the final CDF graphs to obtain the sea level elevation values for the return period of a 200 years. The 200 year event is considered as a realistic worst case scenario criterion for the assessment of the resulting inundation. Equations are then produced to describe the CDF graphs as a function of return periods. These equations are used as inputs into the simulation process to aid with the development of inundation maps.

3.3 Development of Inundation Maps

Development of the inundation maps is performed in ArcGIS (ESRI, 2011) software with the creation of a rasterized base map from Digital Elevation Model (DEM) file. The raster is manipulated into two layers, one that represents elevation and one that represents the surface cover type (land or water.The two layers are then exported using a Python script and imported into the Python module (Python Software Foundation, 2014). A comparison code is then used to simulate the effects of SLR. The data is then converted into maps and imported back into ArcGIS for visual illustration of the results. Figure 7 is an illustration of the methodology used to simulate the effects of SLR.
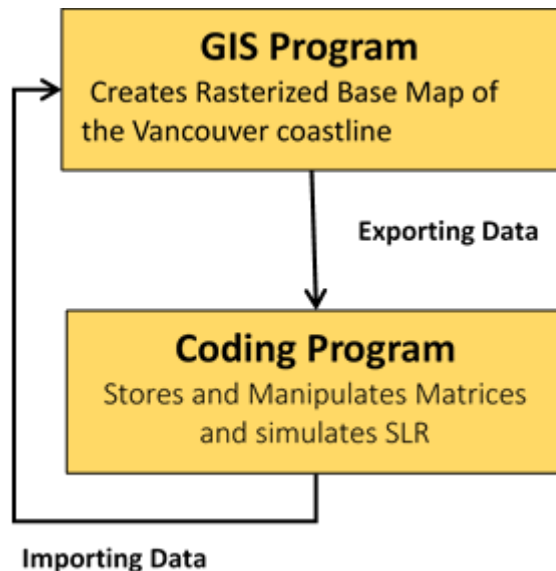
Figure 7 Flow diagram of SLR impacts simulation

3.4 Simulating SLR

For this study a linear simulation process will be combined with GIS software. By utilizing ArcGIS (ESRI, 2011) and its integrated Python (Python Software Foundation, 2014) feature, allowing users to communicate directly with GIS software using the basic code. This allows one to perform the simulation and visualization all through ArcGIS (ESRI, 2011).

To simulate the rising sea level a methodology is created based on the work of Sahin and Mohamed (2010). The methodology is used to identify the impacts and to simulate flooding.

The simulation process relies on a cover matrix, a land elevation matrix and a value of sea level elevation. Using these variables a simulation code is created in Python (Python Software Foundation, 2014) to simulate the process of flooding.

The simulation compares a cell of interest to all adjacent cells and converts a land cell into a water cell if the following two criteria are met:

1. The elevation of the cell of interest is less than the elevation of the adjacent cell

AND

2. The adjacent cell is water.

Figure 8 is an illustration of the general simulation method. The red cell represents the cell of interest, while the blue cells represent the adjacent cells. Given the situation where one of the adjacent cells is water and has a higher elevation than the red cell, the red cell will be "flooded" with water.

i+1,j-1	i+1,j	i+1,j+1
i,j-1	i, j	i,j+1
i-1,j-1	i-1,j	i-1,j+1

Figure 8 Illustration of a generalized simulation method

Boundary Definition

The raster file is in the shape of a rectangle. Because of the rectangular shape three different cases are developed, where each case considers a different number of adjacent cells. The first case looks at the corner cells of the matrix, where the four corners have three adjacent cells. The second case considers the four borders; top, bottom, left and right, these cases have five adjacent cells to be compared with. Finally the last case is created to evaluate all of the internal cells, which are surrounded by eight adjacent cells. Figure 9 illustrates the three different evaluation cases, where the red cell represents the cell of interest.
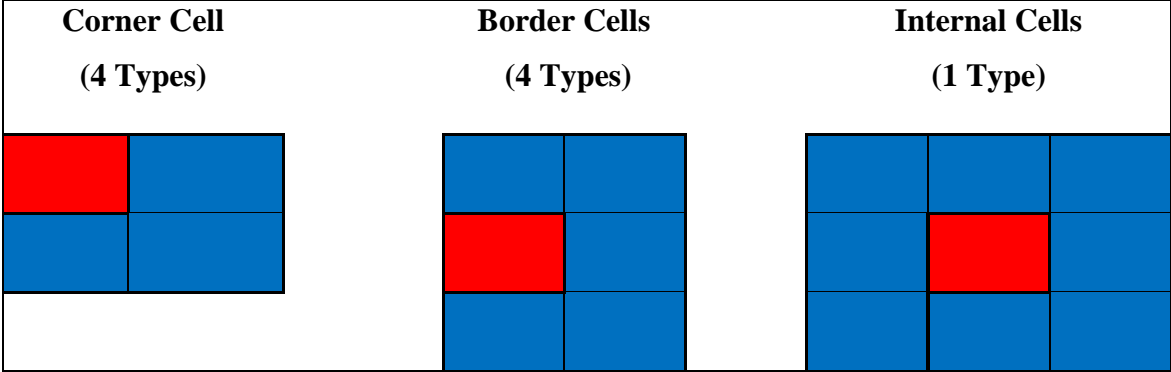
Figure 9 Illustration of different boundary cases

Dynamic Referencing

One requirement of the simulation process is that two out of the three cases require dynamic referencing. In order to evaluate all border and internal cells, the cell of interest has to move across the entire matrix.

This process is coded in Python (Python Software Foundation, 2014), for all three cases. The corner cell code does not need any dynamic referencing and is easy to apply. The border and internal cells code requires dynamic referencing to simulate the rising sea levels. For the four border and one internal types of cells the cell of interest is shifted from left to right and up to down.

Once the simulation code in Python (Python Software Foundation, 2014) is created a variable known as the Sea_Level is defined and set equal to the SLR rate equation. Using different rates, the inundation maps are created for different time periods. For the full Python code see Appendix A .

Creating Elevation Matrix

An elevation matrix is required to define the topography of the region. DEM files are manipulated to gain more detail.

The DEM file is manipulated using the following steps:

1. Copied the CDEM as a raster using the raster copy tool. No data values were set equal to 0.
2. Changed the coordinate system to UTM NAD 1983 Zone 10 to gain the proper spatial referencing. This was done using the Project tool.
3. Changed to integer data type to float using the Float tool
4. Resampled the cell size from 18m by 18m to 5m by 5m to gain further detail. This was done using the Resample tool, setting the resample technique to cubic. This method uses the averages from the 16 nearest cells and was the only interpolation technique that gain decimal values, which was a requirement given the scale of SLR.

Figure 10 is an example of an elevation raster. Figure 11 is an example of the float type data found in the raster file.
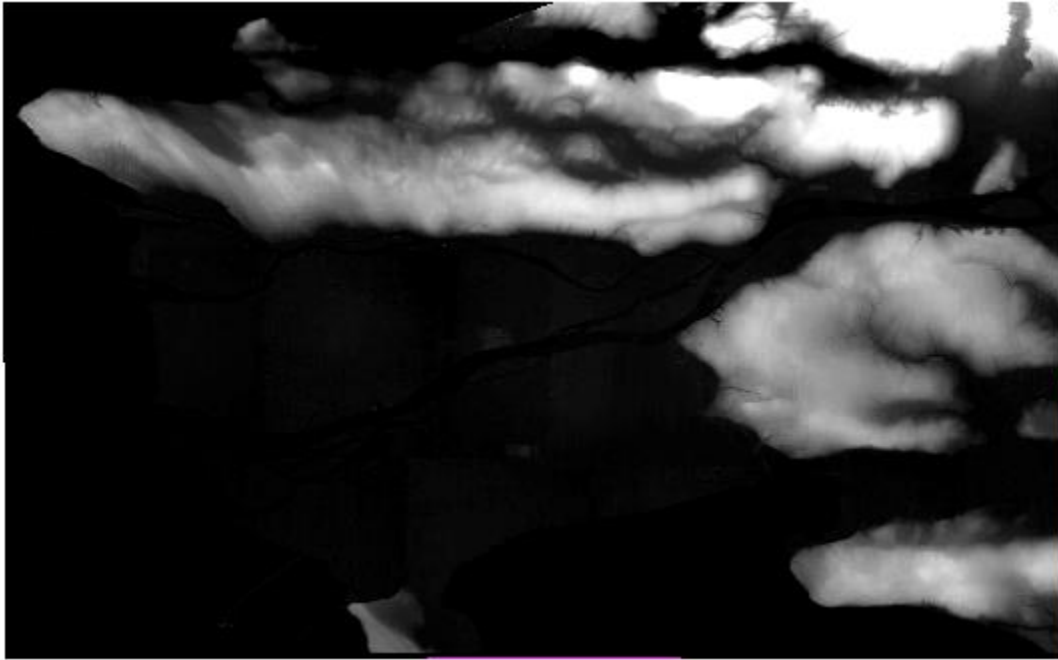
Figure 10 Elevation raster

	0	1	2
0	100.06400299072266	100.07199859619141	100.039810180066406
1	100.14800262451172	100.06462860107422	99.902069091796875
2	100.3291015625	100.1412353515625	99.829643249511719
3	100.54323577880859	100.24252319335937	99.769844055175781
4	100.72740936279297	100.32354736328125	99.703338623046875
5	100.82874298095703	100.33232879638672	99.579010009765625
6	100.82280731201172	100.26752471923828	99.428886413574219
7	100.77700042724609	100.17350006103516	99.264434814453125
8	100.70637512207031	100.06256103515625	99.093658447265625
9	100.67334747314453	100.01722717285156	99.028800964355469
10	100.68921661376953	100.04404449462891	99.0689697265625

Figure 11 Elevation values found in the raster file

Creating Cover Matrix

A cover matrix is required to define areas of water or land, where 2 is defined as water and 0 as land. To create the cover matrix the entire elevation matrix is changed to represent land values.

22

This requires changing the raster properties so that all values of the matrix are 0. This is done using the following steps in ArcGIS:

1. Converted CDEM raster from float data type to integer data type using the int function in ArcGIS. This step is essential as it allows the user to view the attribute table of the data which is required for manual manipulation of the raster.
2. Added another field in the attribute table, done using the Editor function in ArcGIS. The field was labelled as "Cover"
3. Manually edited all Cover values to 0 using the Editor function
4. Created a new raster with Cover values equal to 0 using the Lookup function

A water shape file is then used to define the coastline. The shape file is used to cut the cover matrix, where cells defined as water are changed to 2 and cells defined as land are left as 0. The Clip tool was utilized to perform this task. Figure 12 is an image of a cover raster file with the overlaid water shape file.
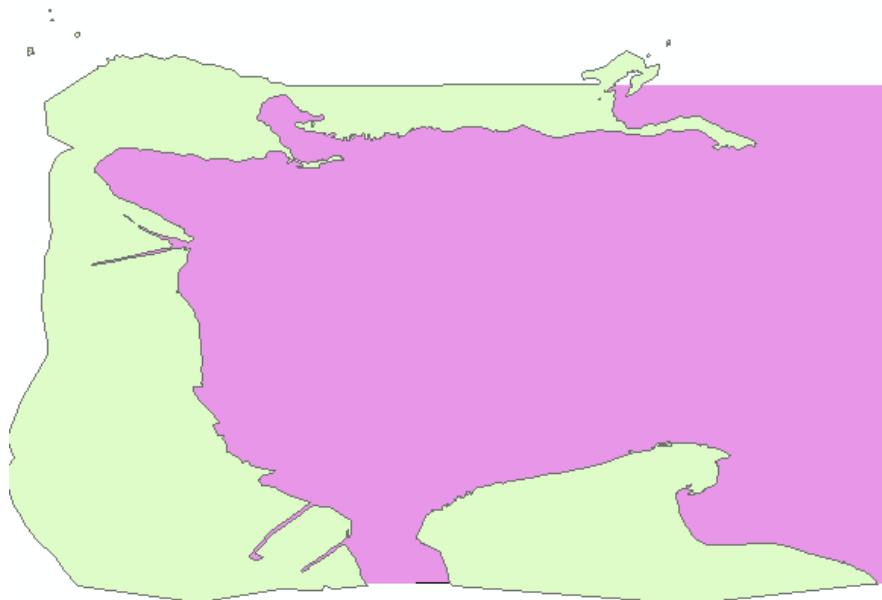
Figure 12 Blank cover matrix with overlaid water shape file

A cover raster is constructed using the steps above. Figure 13 shows an example of a cover raster, where land is defined as 0 (white) and water defined as 2 (black).

Figure 13 Cover matrix

3.5 Explanation of SLR Simulation Code

The SLR simulation code uses both ArcGIS (ESRI, 2011) and its integrated Python feature (Python Software Foundation, 2014). All the Python (Python Software Foundation, 2014) code is written in a separate Python Shell and can be found in Appendix A. To access the ArcGIS library of functions a "import arcpy" code is used at the beginning of the script. This allows Python to directly access ArcGIS. The next step is to import both the elevation raster and the cover raster. This is done by converting the rasters to a number array using the "RasterToNumPyArray" function. A variable called "Sea_Level" is then created and set equal to the values gained from both the deterministic and probabilistic analysis. The purpose of the code is to create a new cover raster (Cover_Raster) that captures the areas of land that are less than the sea level elevation value.

The script is then split into 3 different categories; corner code, border code and internal code. These 3 different codes are used to simulate SLR for their respected categories. All categories

follow the same logic where the cell of interest is first determined to be land or water (0 or 2). If the cell is land (0) then the code moves to a comparison statement. The comparison statement looks at the surrounding cells, if there is a cell that is touching the cell of interest and is water (2) and the sea level elevation value is higher than the land elevation of for the cell of interest, then the cell of interest will be converted from 0 to 2 and passed to the Cover_Raster raster. This simulation is done for all categories. The only difference between categories is that the border code and internal code require dynamic referencing. This is done with a for statement. For the border code a for statement is used to loop through the different columns or rows, depending on the borer. For the internal code a for statement is used to loop through both the columns and rows, ensuring that the simulation process is performed for all cells. To loop through columns and rows the following expressions are used, respectively: "for colNum in xrange(1,7684):" , "for rowNum in xrange(1,7072):"

The final portion of the script is used to pass the spatial description to the new Cover_Raster raster. This is done by extracting the spatial information from a raster that is already created and passing this information to the new raster. The final step is to save the raster into a folder of the users choice.

4. Case Study

   The province of British Columbia has a population of 4,400,057 where 80% of this population lives within 5 km of the coast. The Lower Mainland is where most of the population resides. Over 4,600 hectares of farmland and over 15,000 hectares of industrial and residential areas in the Lower Mainland are located within 1 m of sea levels (The Arlington Group Planning and Architecture Inc. et al., 2013). For this case study the area of interest covers Metro Vancouver. This area is highlighted in red in Figure 14**.**
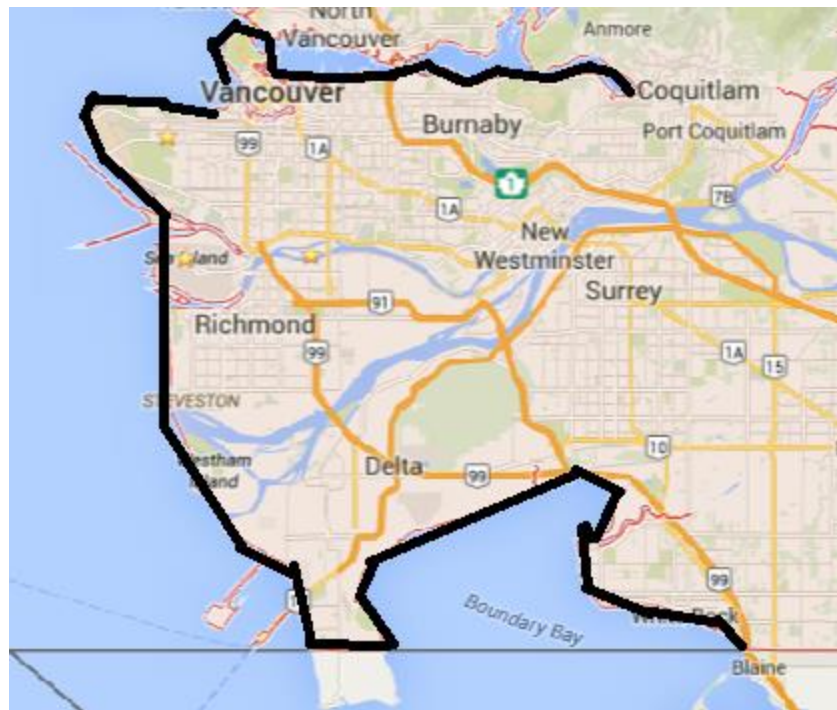
Figure 14 Case study area

4.1 Input Data

   For this case study there were many types of input data required for the analysis. The first data set includes hourly tidal gauge data .The tidal gauge data for Vancouver was downloaded from the web (http://www.isdm-gdsi.gc.ca/ - last accessed November 2014). Hourly data resolution is selected for capturing the details of historical extreme events. The tidal gauge data is available

from 1909 - present, however due to a lack of data from the years 1923-1942, the period 1943 - 2013 is actually used. Figure 13 illustrates the location of the tidal gauge station.

The second input includes the elevation data which comes in the form of a single DEM file. The data is known as a Canadian Digital Elevation Model (CDEM). This type of data is also referred to as digital surface model, meaning any structure located on the surface of the Earth is also included in the dataset. It is important to use this type of data rather than the digital terrain model which only includes the topography of the land. The digital surface data include most of the structures (dikes, barriers, etc) that play a significant role in the development of the inundation maps. One issue that arises from using a digital surface model is that the building elevations are mapped in the DEM file from the top of the building, therefore the ground level of the building may be flooded with water but the simulation process will not recognize this as the elevation is set to the building's roof top and not the actual ground. Figure 15 is an example of this data. The CDEM file has a horizontal cell resolution of 18.5m by 18.5m, and a vertical accuracy on the scale of 5-15m.For more detail regarding the accuracy and validity of the data see Appendix B.
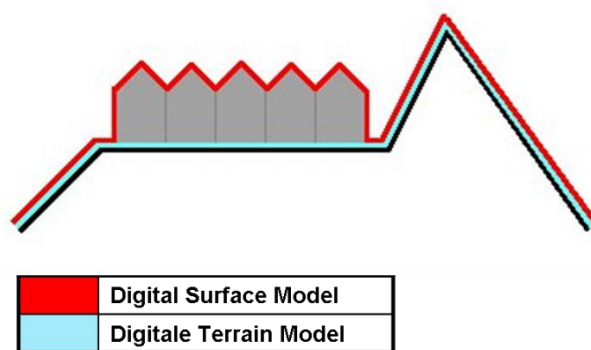
Figure 15 Illustration of difference between the digital surface model and digital terrain model

Figure 16 is illustration of the CDEM data obtained from the Natural Resources Canada Geo Gratis (http://geogratis.gc.ca/site/eng/extraction - last accessed November 2014)
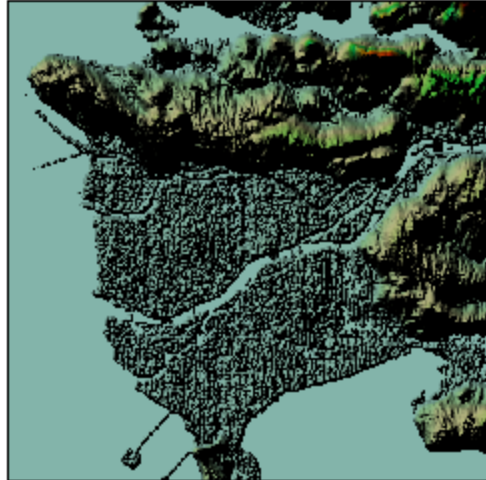
Figure 16 CDEM file for the Vancouver coastline

The third input are the IPCCs SLR rates. These rates were used as the base rates for both, the deterministic and probabilistic analyses. To create regional SLR rates these global rates were adjusted to factor in the regional considerations. These rates were extracted from the main documentation of the IPCC AR5 (Church et al, 2013). Table 2 presents the global rates for the location of case study.

Table 2 IPCC SLR rates

Scenario	Rate (mm/year)
RCP2.6	4.4
RCP4.5	6.1
RCP6.0	7.4
RCP8.5	11.2

The final input data include the rate of VLM. The topography in Vancouver is lifting which is working in the same direction as SLR. The Ausenco Sandwells report (2011) states that the area

of Vancouver is experiencing an uplift of 1.2 mm/year. This rate is used to adjust the global rates of SLR to regional rates.

4.2 Analysis

Deterministic Method

The deterministic method starts with the use of the IPCCs global rates of SLR. The IPCC projections of SLR rates are available up to the year 2100 for four emission scenarios known as RCP2.6, RCP4.5, RCP6.0 and RCP8.5. Figure 17 presents the different SLR rates for all scenarios.
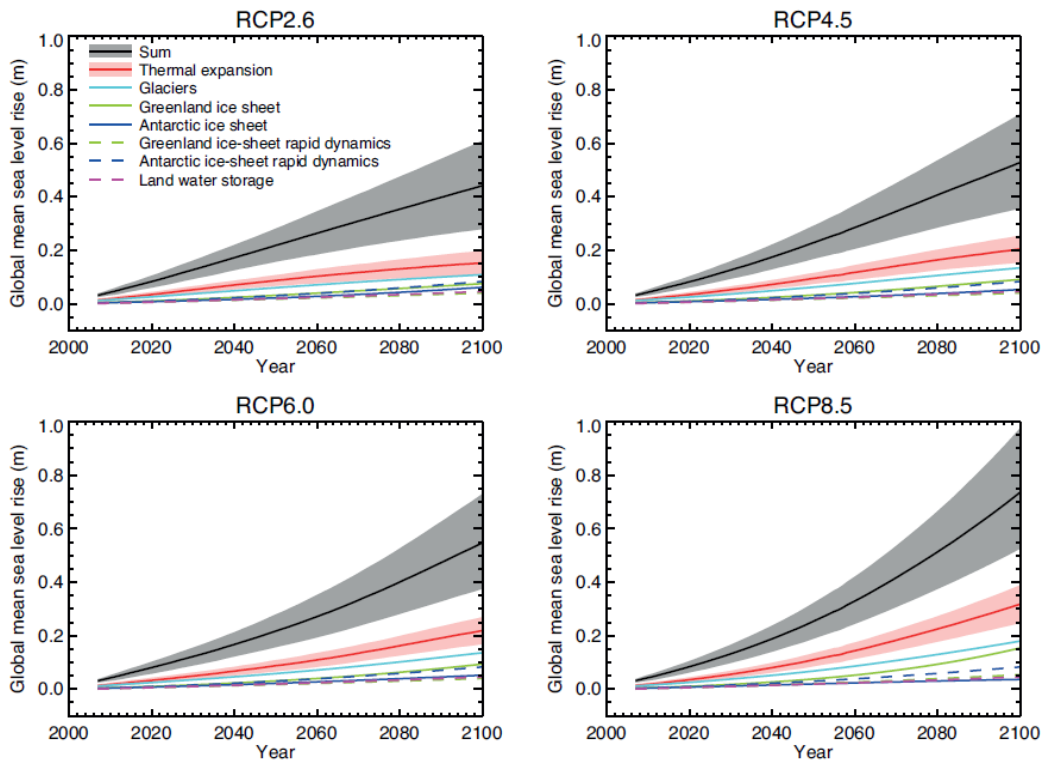
Figure 17 IPCC SLR rates
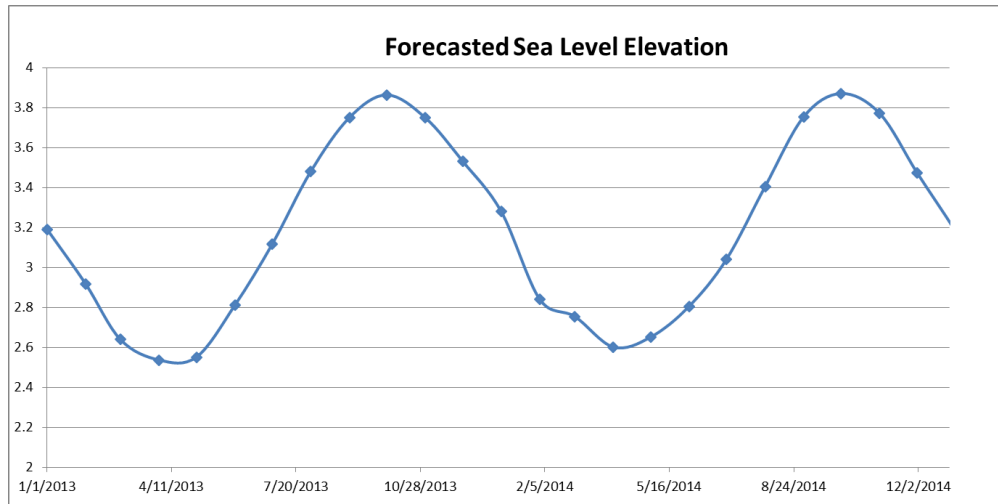
Figure 18 Forecasted sea level elevation for the Metro Vancouver

These global rates are adjusted to factor in the regional considerations of local tidal movements and VLM. U_Tide (Codiga, D.L., 2011) was utilized to forecast the sea level elevation for Vancouver .Using the ut_reconstr() function a forecast is created for Vancouver's local tidal patterns for the next 100 years. Figure 18 is a snapshot of the forecasted data graph. For details on the options selected through the analysis stage see Appendix C.

  In terms of VLM, the topography of Vancouver is lifting which is working in the same direction as SLR. Therefore the VLM rate of 1.2 mm/year, is subtracted from the rates of SLR to adapt. From this the global SLR rates are adjusted to the local conditions in Vancouver.

  Using the IPCC rates along with the natural tidal movement and VLM the different regional rates of SLR for the next 100 years are developed and shown in Figure 19.
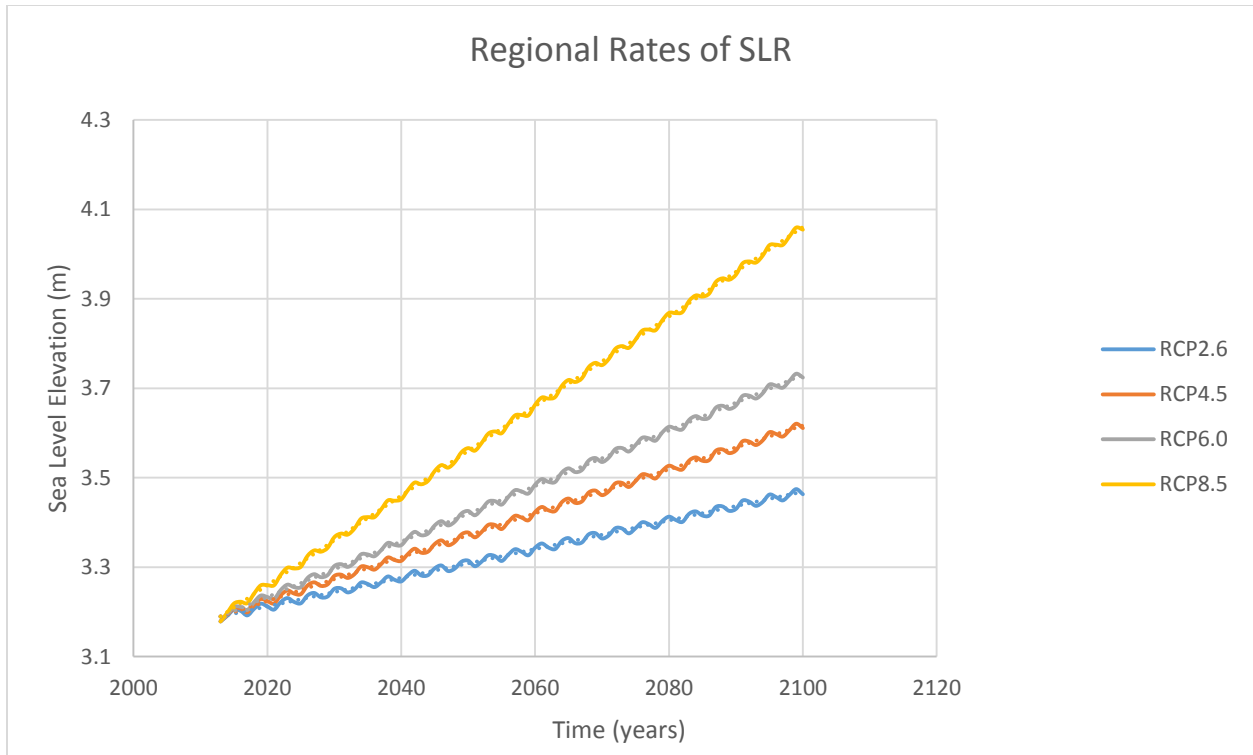
Figure 19 Regional rates of SLR for the Metro Vancouver coastline

The rates are linearly approximated to obtain the mean rate of SLR. The corresponding equations are presented in Table 3.

Table 3 Regional SLR rates for different emission scenarios

Scenario	Equation
RCP 2.6	y = 0.0038x - 4.4301
RCP 4.5	y = 0.0049x - 6.6824
RCP 6.0	y = 0.0062x - 9.2993
RCP 8.5	y = 0.01x - 16.949

The probabilistic method starts with the use of hourly tidal gauge data. The data is then detrended using three different methods. For all three methods the following steps are implemented in the implementation of the probabilistic method: (i) data download; (ii) graphical analyses of data to obtain liner equations; and (iii) detrending the data by taking the difference between the Original Sea Level Elevation and Linear Regression of Sea Level Elevation (Teetor, 2011).

The first method of detrending the data is using a basic linear approximation. This is the only method that uses the raw hourly tidal gauge data. Figure 20 shows the natural sea level variability with the mean at the 3m elevation mark.
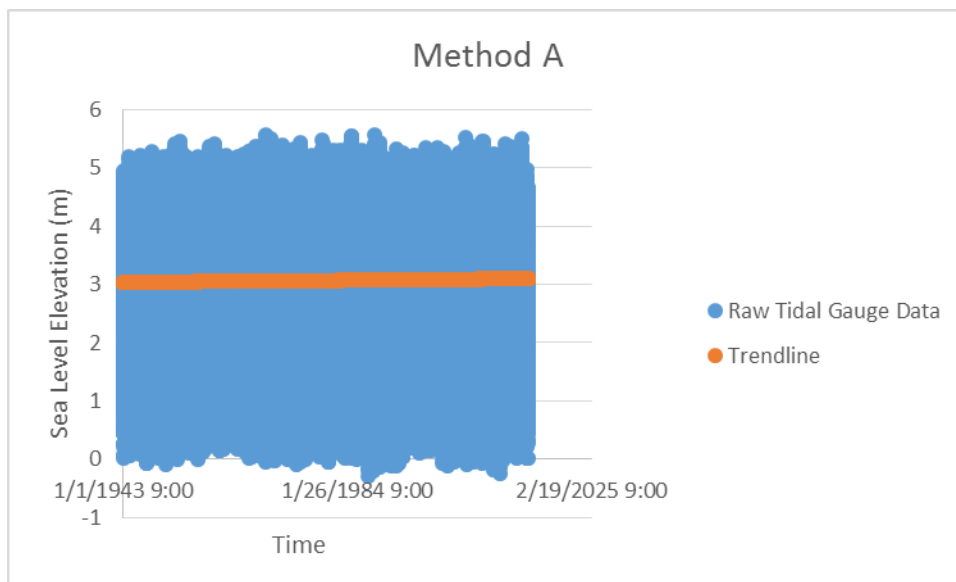
Figure 20 Detrending method A: linear fit

The second method of detrending the data uses a 19 year moving average of the tidal gauge data. The hourly data is averaged to a yearly timescale. The purpose of a 19 year moving average is to incorporate the astronomical tidal trends. Every 18.6 years a lunar cycle is completed. This cycle plays a role in determining the astronomical tide for a given region.

Therefore, by using a 19 year moving average a lunar cycle is properly considered (Denny and Paine, 2008). Figure 21 displays the 19 year moving average as well as its liner approximation.
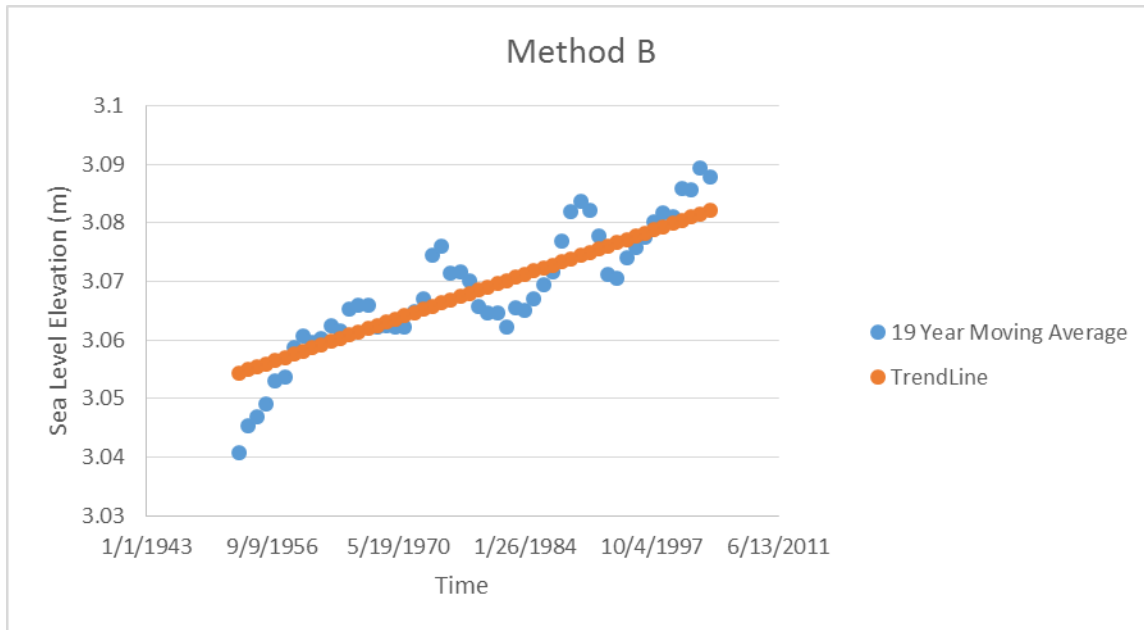
Figure 21 Detrending method B: 19 year moving average

The third and final method of detrending the data uses a 1 year moving average. This method properly removes the long term trend and address the seasonality of the data (Arns et al, 2013). Figure 22 illustrates the data used in the analysis and their linear approximations.
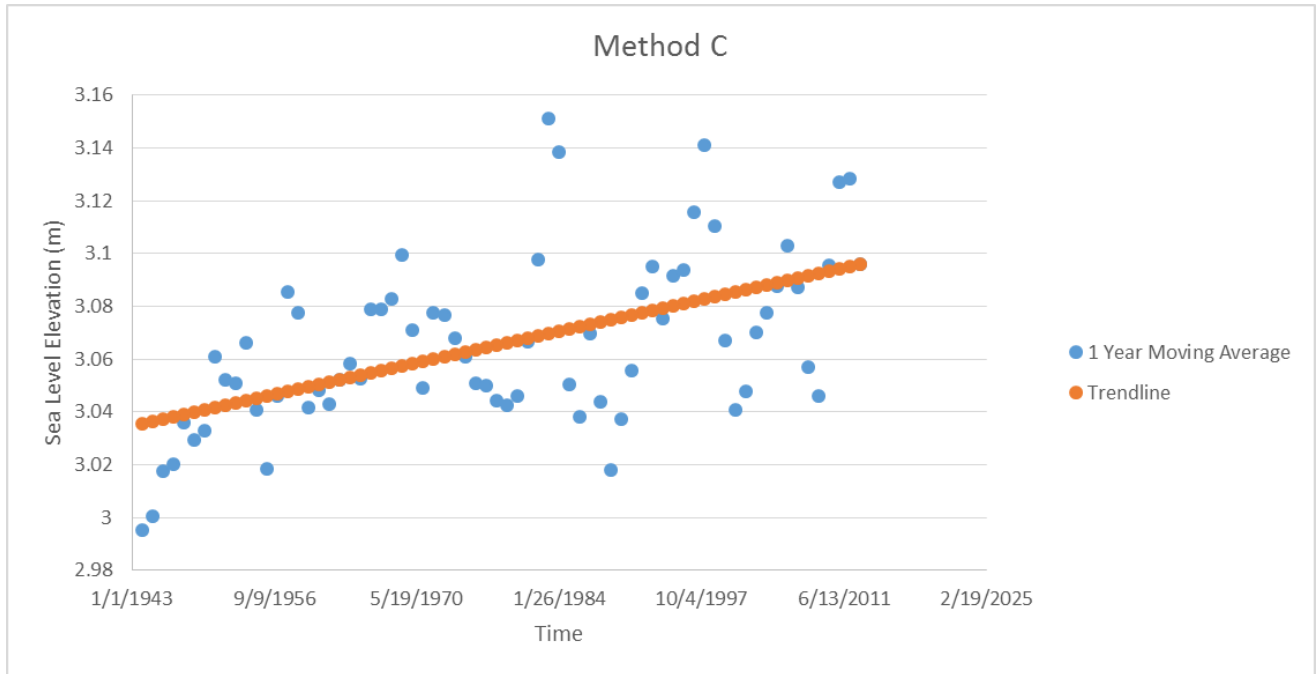
Figure 22 Detrending method C: 1 year moving average

When comparing Figure 20 to Figures 21 and 22 a less dominating trend is visually present. The three methods were utilized to detrend the data. One method is subjectively selected based on the final results.

Once the data is detrended the next step is to apply the BM method. The values are first separated according to season, then maximum values are found for each season. Finding the largest values per season was done using a Excel macro code. See Appendix D for details and the code used for the implementation of block maxima method.

MLE parameters are estimated using the gevfit(x) function in Matlab (MATLAB 7.1.2, 2011). This was done for all three detrending methods and for all seasons. Figure 23 shows an example of the MLE parameters obtained for the winter season and detrending method A. The code used to find the MLE parameters is provided in Appendix E.

Maximum Likelihood Estimation (MLE)
R=1

Parameter	Value	95% CI Intervals	
Shape Parameter (ξ)	- 0.3636	- 0.5127	- 0.2144
Scale Parameter (σ)	0.1644	0.1371	0.1971
Location Parameter (μ)	2.1403	2.0984	2.1822

R=2			

Parameter	Value	95% CI Intervals	
Shape Parameter (ξ)	- 0.3374	- 0.4246	- 0.2502
Scale Parameter (σ)	0.162	0.1432	0.1833
Location Parameter (μ)	2.0998	2.071	2.1287

R=3			

Parameter	Value	95% CI Intervals	
Shape Parameter (ξ)	- 0.3107	- 0.3787	- 0.2426
Scale Parameter (σ)	0.1609	0.1456	0.1778
Location Parameter (μ)	2.0665	2.0431	2.0899

R=4			

Parameter	Value	95% CI Intervals	
Shape Parameter (ξ)	-	-	-0.227

Parameter	Value	95% CI Intervals	
		0.2858	0.3445
Scale Parameter (σ)	0.1583	0.1452	0.1726
Location Parameter (μ)	2.0413	2.0213	2.0612

R=5			
Parameter	**Value**	**95% CI Intervals**	
Shape Parameter (ξ)	-0.2646	-0.3178	-0.2115
Scale Parameter (σ)	0.1558	0.1442	0.1683
Location Parameter (μ)	2.0201	2.0025	2.0377

R=6			
Parameter	**Value**	**95% CI Intervals**	
Shape Parameter (ξ)	-0.2482	-0.2976	-0.1988
Scale Parameter (σ)	0.1542	0.1436	0.1655
Location Parameter (μ)	2.0016	1.9857	2.0175

Figure 23 Maximum likelihood estimation parameters for winter season and detrending method A

Once MLE parameters are known the next step is to fit the data to a GEV distribution. Again this was done for all detrending methods and all seasons. Figure 24 is an example of a cumulative density function (CDF) developed for detrending method A, the winter season, and R=1.
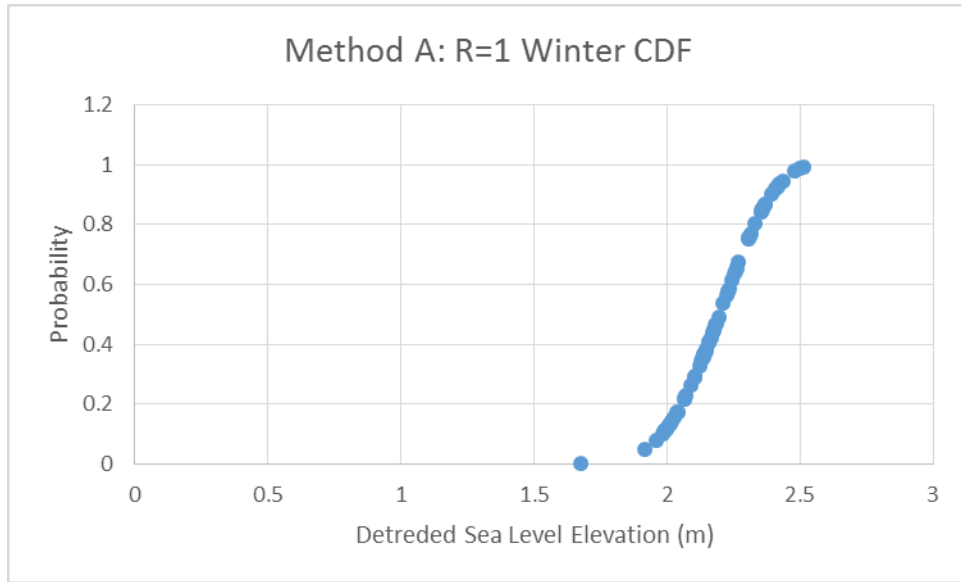
Figure 24 CDF for method A: winter season and R=1

CDF graphs were calculated for all detrending methods and all seasons. Figures 25, 26 and 27 are showing the results for all three detrending methods for the winter season.
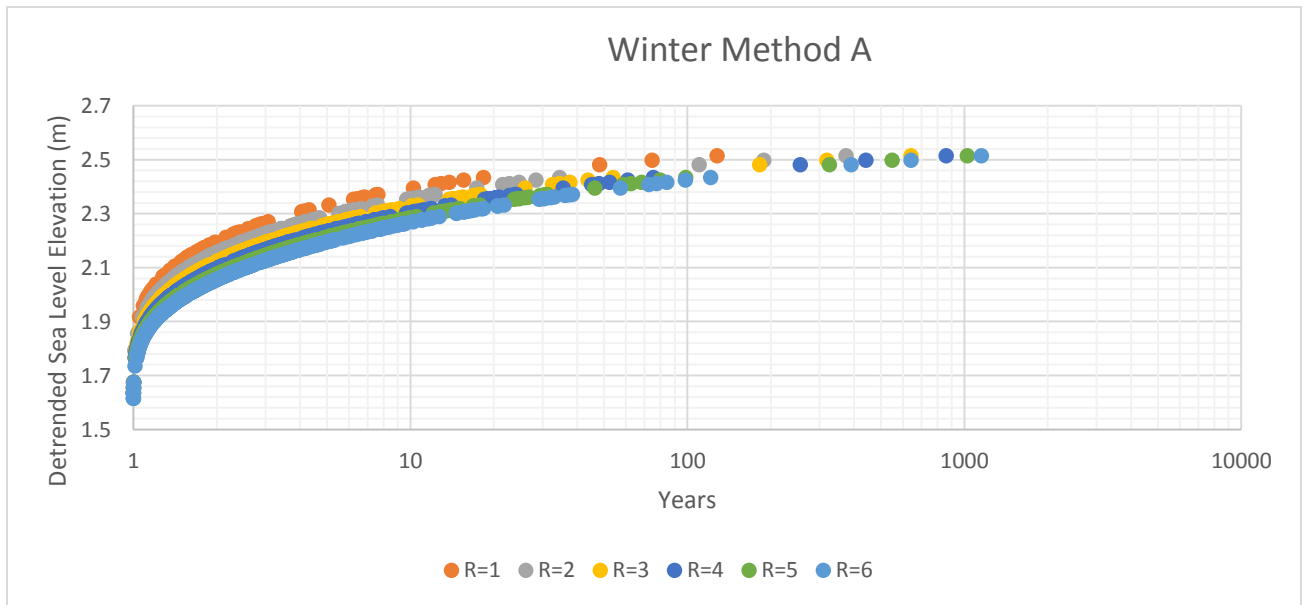
Figure 25 CDF graph: winter season and detrending method A
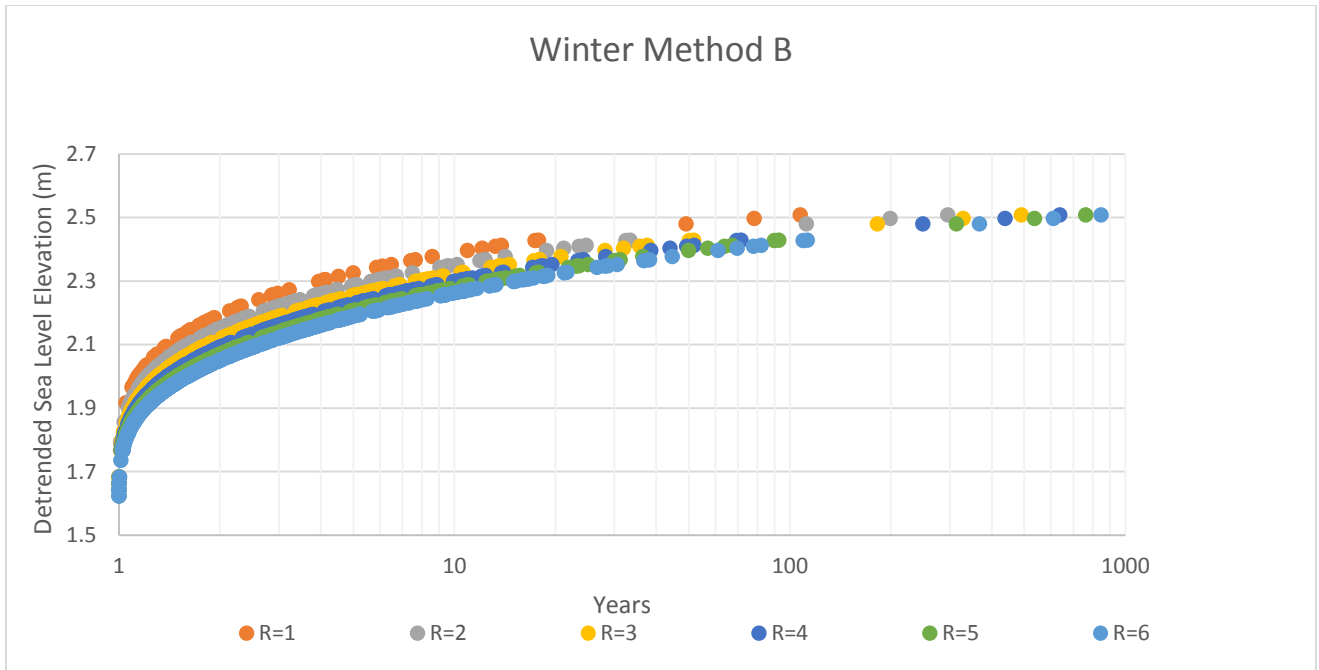
Figure 26 CDF graph: winter season and detrending method B
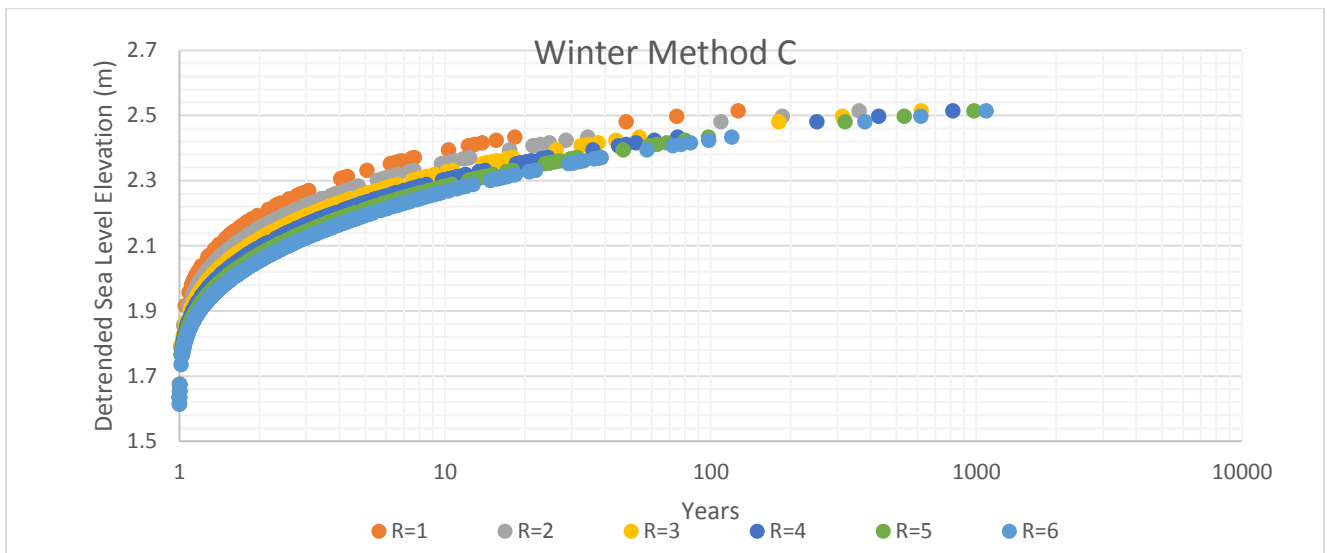
Figure 27 CDF graph: winter season and detrending method C

Comparison of the three detrending methods shows a very small difference. Method B is selected to be the final detrending method. This choice is justified by the 19 year moving average and its relationship to the 18.6 lunar cycle. In terms of the final R value, the value of 1 is selected

due to the fact that it consistently results in higher return period values for all detrending methods. By using R=1 only one maximum value per block was used, this ensures that only one extreme event was considered, as opposed to using R=6 where 6 events are considered 5 of which may not be considered extreme at all. Therefore using R=1 filters through the data, leaving only the largest possible events.

Comparison between the seasons shows a larger difference. From Figure 28 it is obvious that the highest sea level elevation for a given return period is obtained during the winter season. The summer season shows the lowest sea elevation. To capture the natural variability of the tides, both winter and summer season results are utilized.
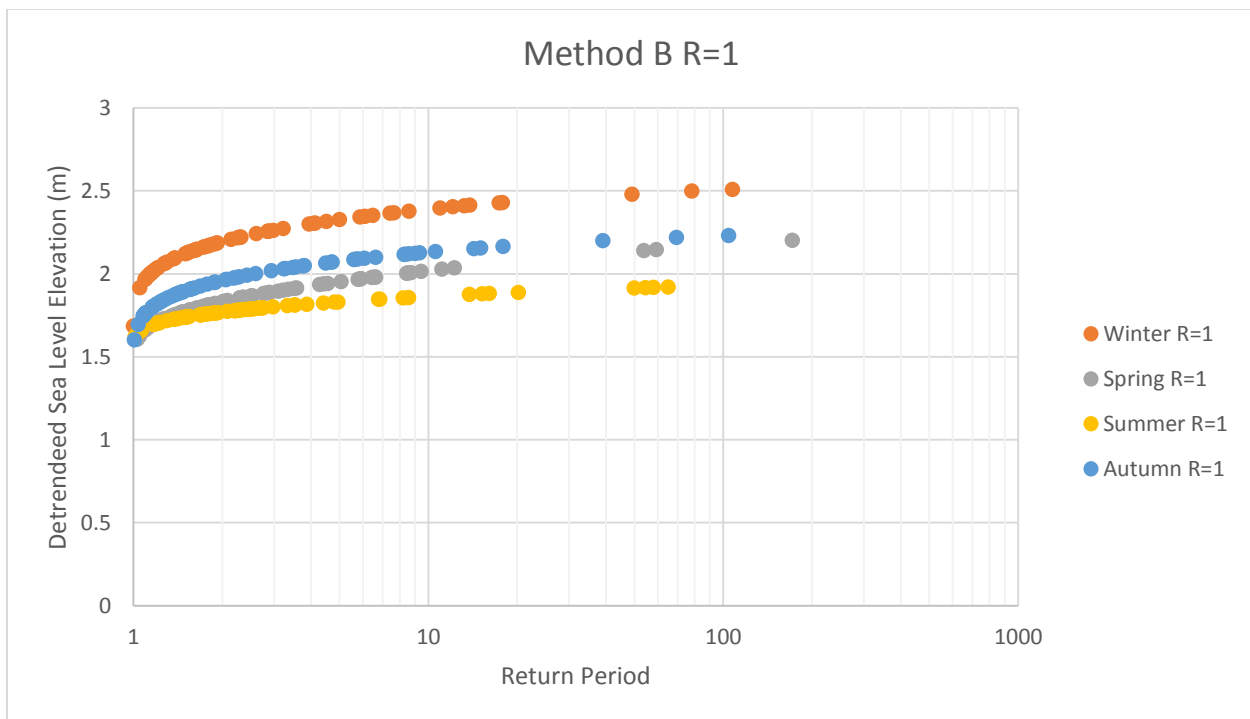
Figure 28 CDF graph: detrending method B and R=1

Therefore the final selection of methodological steps results in the following:

- Detrending Method: B
- R value: 1

- Maximum Season: Winter
- Minimum Season: Summer

Figure 29 shows the final results for the selected modeling parameters.
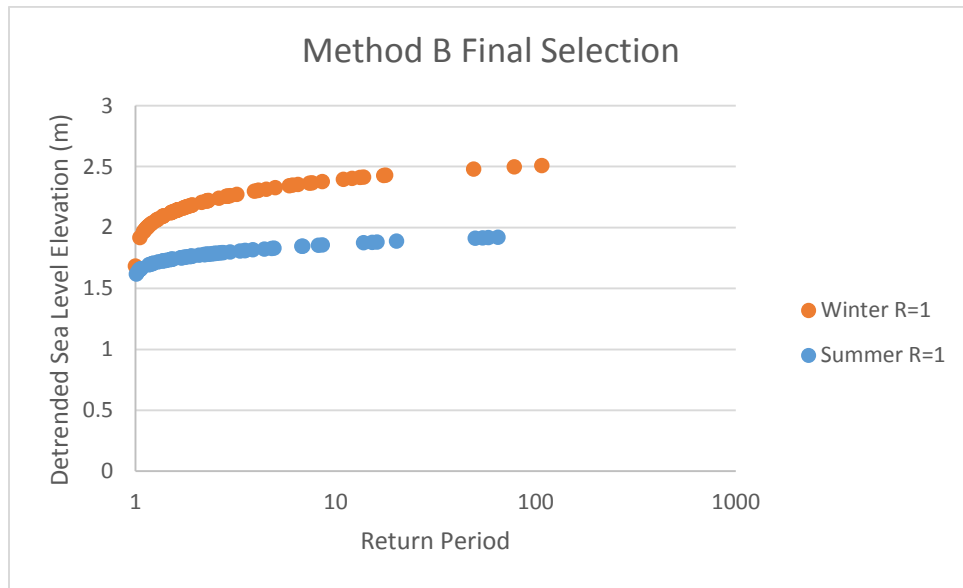
Figure 29 The final CDF graph

   Once the final CDF graphs were created the final step is to incorporate SLR with the CDF graphs. To gain a better understanding of the effects of sea level rise and assess the change in frequency pre 1960 data is compared to post 1960 data. The year 1960 was used to match the analysis done by John Hunter and John Church (Church *et al*, 2008). They used the year 1950, however due to lack of data the year 1960 was used in the research presented in this study.

   Figure 29 shows the comparison of the pre and post 1960 return periods for the winter season. Due to sea level rise the events post 1960 occur at a higher magnitude and more frequently. This is also the case in the comparison of the pre and post 1960 data for the summer season.
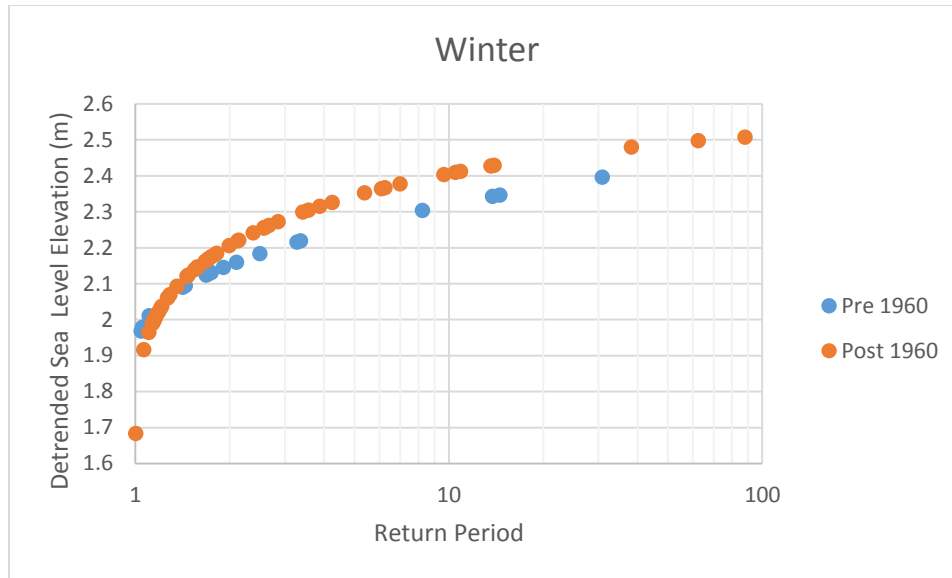
Figure 30 CDF graph: winter season pre 1960s and post 1960s
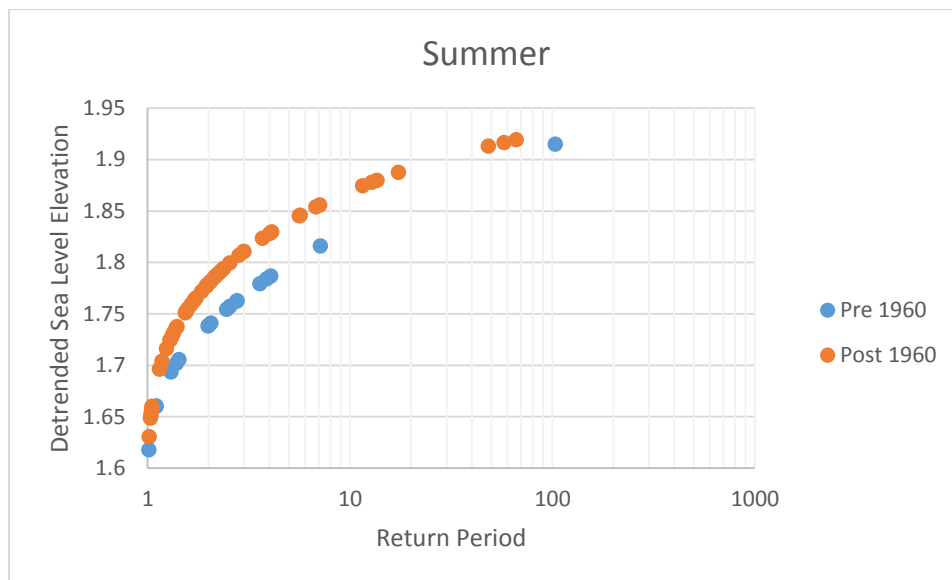
Figure 31 CDF graph: summer season and pre 1960s and post 1960s

In general Figures 30 and 31 display ideal results. The graphs show that the pre 1960 events occur less frequently than those post 1960. It also shows that the events that do occur at the same frequency are at a higher magnitude for the post 1960 era when compared to the pre 1960s. This observation will be used to develop a factor that depends on both the increase in magnitude as well as the increase in frequency (Church *et al*, 2008).

To develop this factor an important assumption was made. Since the sea level varies logarithmically with the average return period this indicates that the relationship approximately follows a Gumbel distribution (Church *et al*, 2008).

For winter and summer seasons for return periods under a 1.1 year the pre 1960 events appear to happen more frequently than post 1960 events. For the development of the equation data past the return period of a 2 years was considered. The justification for this is that the more extreme return periods are of interest.

Using the pre 1960s and post 1960s frequency distributions the r and h values are found. The h value is determined by taking the difference between two points of approximately the same return period. The value of r is determined by finding the quotient between two points of the same magnitude. Figure 32 illustrates the procedure in graphical form. The h value in this case is found to be .0845 and the r value is 2.31.
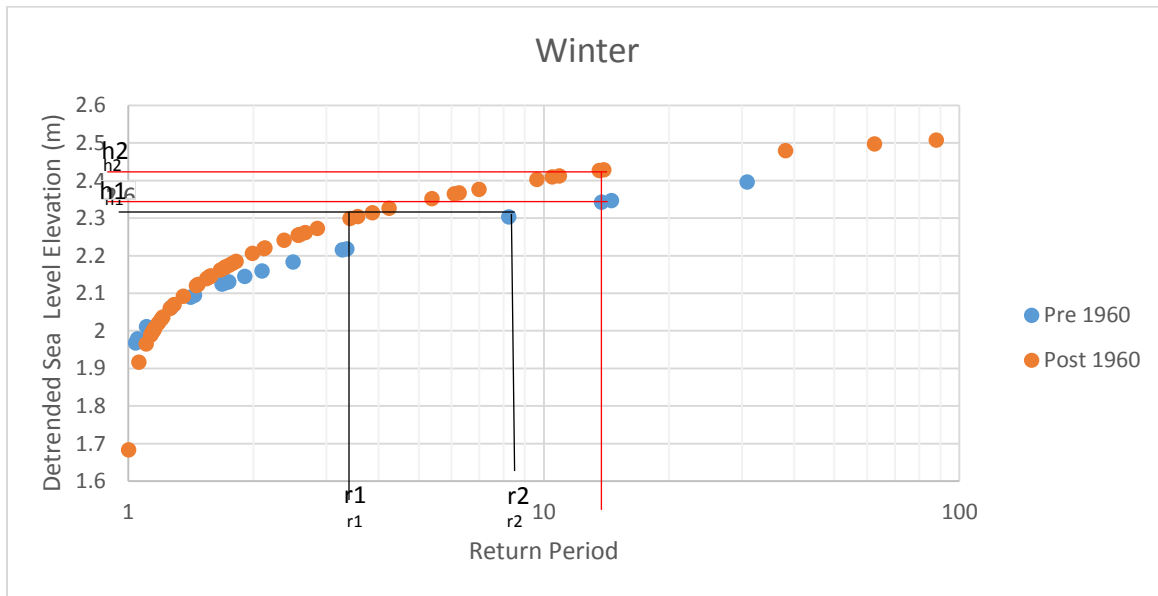
Figure 32 CDF graph: development of the factor for winter

The final values for r and h are presented in Table 4 for both, summer and winter seasons.

Table 4 Final r and h values

	Winter		Summer
r	2.310	r	2.389
h	0.0845	h	0.0441

The IPCC rates are then added on to the 2013 sea level average to gain sea level elevations up to the year 2100. Table 5 is a summary of all the projected sea level elevation values.

Table 5 SLR projections relative to 2013

IPCC Sea Level Rise Projections						
Scenario	Rate (mm/year)	$2013_{Average}$	2015	2025	2050	2100
RCP2.6	4.4	3.045	3.054	3.098	3.208	3.428
RCP4.5	6.1	3.045	3.057	3.118	3.270	3.575
RCP6.0	7.4	3.045	3.060	3.134	3.319	3.689
RCP8.5	11.2	3.045	3.068	3.179	3.459	4.019

Before the value of H could be calculated the influence of VLM is factored in, by subtracting the VLM rate from the SLR rate.

Once the sea level elevation values are calculated relative to 2013, the values are then back calculated to find the actual increase since 2013, which is the value of H, as presented in Table 6.

Table 6 Finalized H values

H value (m) - Considering VLM

Scenario	2015	2025	2050	2100
RCP2.6	0.0076	0.0516	0.1616	0.3816
RCP4.5	0.011	0.072	0.2245	0.5295
RCP6.0	0.0136	0.0876	0.2726	0.6426
RCP8.5	0.0212	0.1332	0.4132	0.9732

After the values of H are determined, the next step is to calculate the value of $r^{H/h}$, using r and h from the pre and post 1960s graphs. This is done for all RCP scenarios and time scales. Tables 7 and 8 show the final $r^{H/h}$ values for winter and summer respectively.

Table 7 Finalized ratios for winter season

Scenario	$r^{H/h}$ value Winter			
	2015	2025	2050	2100
RCP2.6	1.0782	1.6674	4.9589	43.859
RCP4.5	1.1151	2.0409	9.2480	189.89
RCP6.0	1.1443	2.3820	14.894	582.33
RCP8.5	1.2337	3.7426	59.985	15409

Table 8 Finalized ratios for summer season

Scenario	$r^{H/h}$ value Summer			
	2015	2025	2050	2100
RCP2.6	1.1619	2.7701	24.311	1872.5

RCP4.5	1.2426	4.1442	84.178	34732
RCP6.0	1.3081	5.6391	217.61	324054
RCP8.5	1.5198	13.8758	3494.6	2E+08

The final step is to increase the post 1960 return period values to incorporate the effects of sea level rise and assess the change in frequency and magnitude of the mean sea level. To achieve these two goals, two main steps are required:

- increase the post 1960s sea level elevation data by adding the value of H
- reduce the return period by dividing the return periods by $r^{H/h}$

By completing both steps the effects of SLR are incorporated into the CDF graphs.. Due to climate change in the future storms will occur more frequently and at a higher magnitude. This factor incorporates this increase into the adjusted CDFs.

The final CDF graphs are created by modifications described in the previous section. Again, this is done for both the winter and summer seasons and all emission scenarios. Figures 33 and 34 display the revised return periods for the winter and summer seasons for the RCP2.6 scenario, respectively. For all CDF graphs see Appendix F.
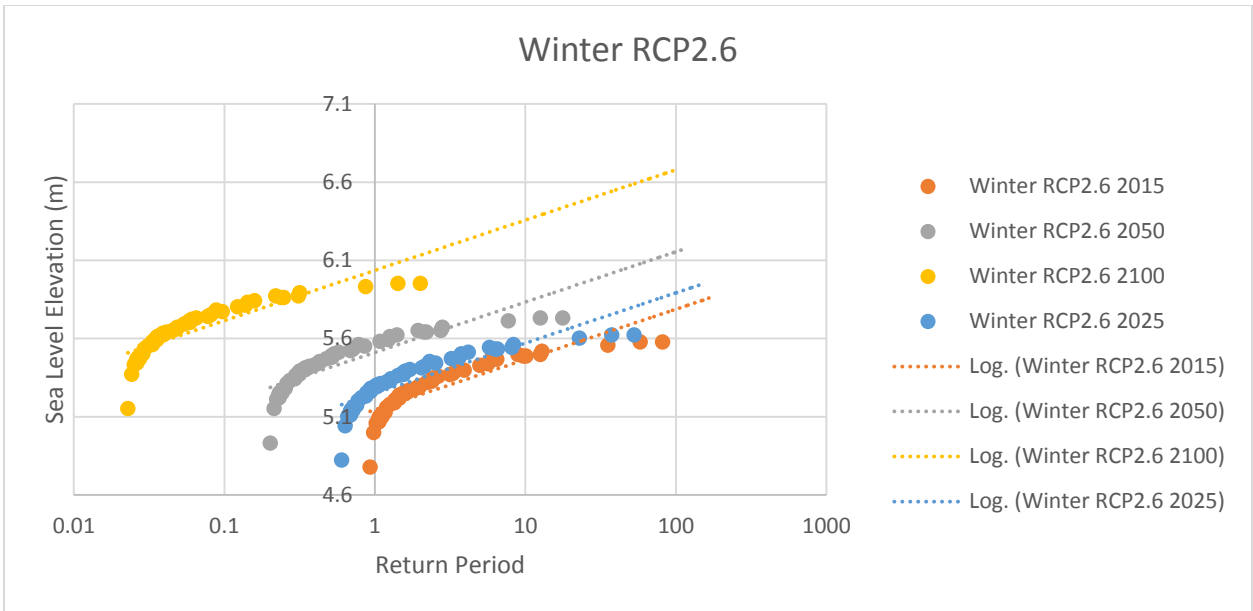
Figure 33 Final CDF graphs: winter season and RCP 2.6
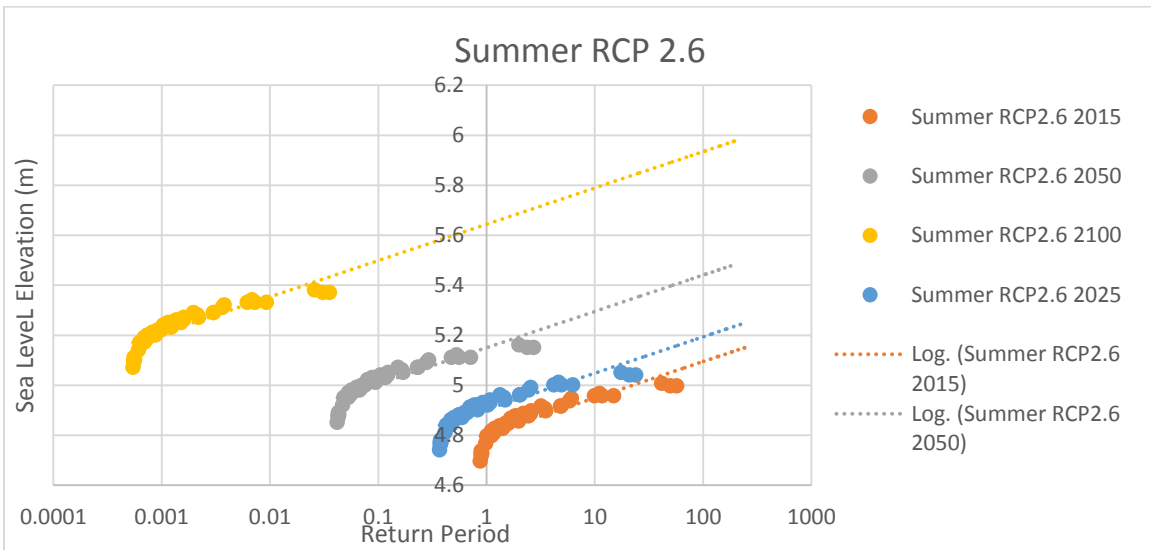
Figure 34 Final CDF graphs: summer season and RCP 2.6

The results are as expected, showing the maximum change for the Winter RCP 2.6 2100 scenario. When comparing Figures 33 and 34 it is obvious that the winter months act as the maximum boundary and summer as the minimum boundary of potential change. A logarithmic extrapolation was performed up to the return period value of 200 years. This procedure is performed for all scenarios for both seasons creating multiple CDF graphs. Figures 35 and 36 show results for RCP scenario 8.5 for both seasons.
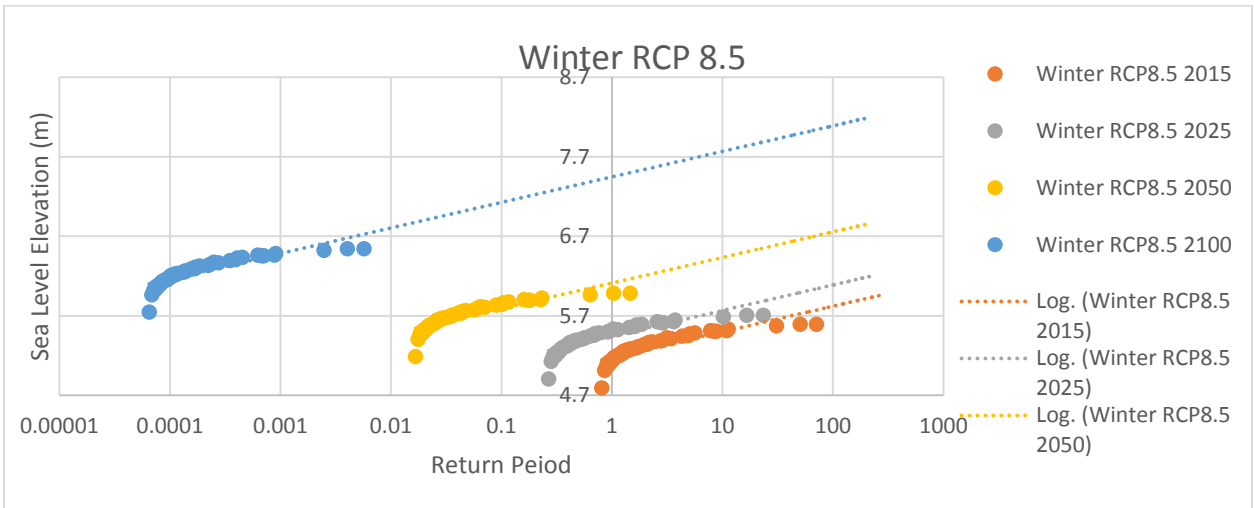
Figure 35 Final CDF graphs: winter season and RCP 8.5
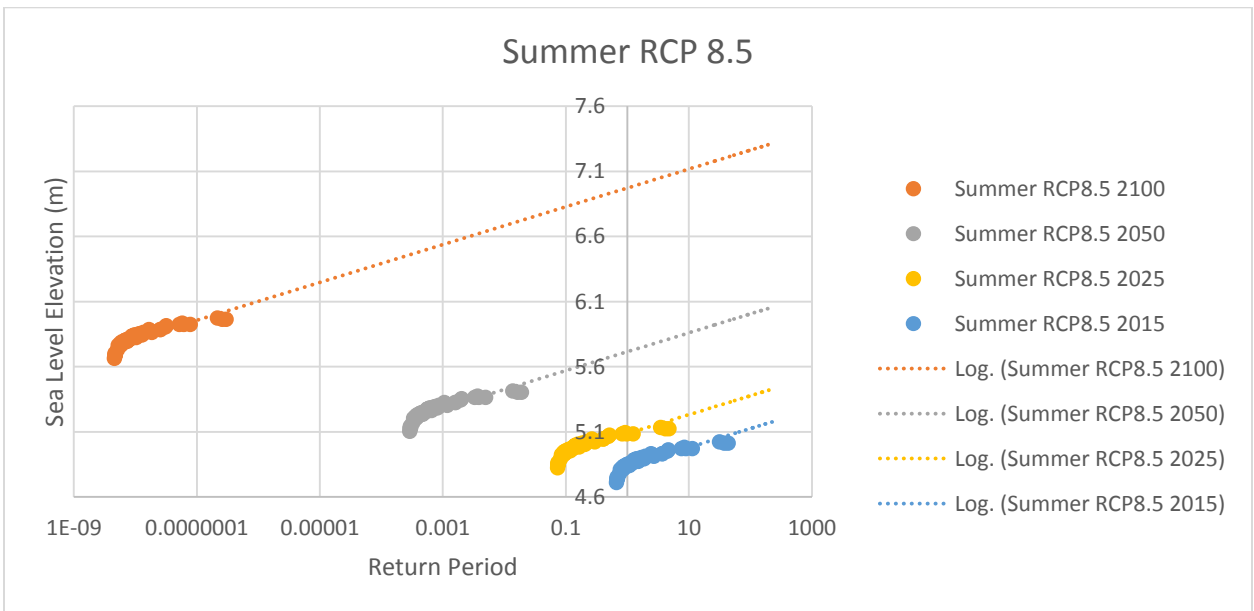
Figure 36 Final CDF graphs: winter season and RCP 8.5

The following equations are used to define SLR rates as a function of the return period for winter and summer seasons, considering RCP scenarios 2.6 and 8.5:

Table 9 Winter and summer RCP 2.6 logarithmic equation

Season	Scenario	Timescale	Logarithmic Equation
Winter	RCP 2.6	2015	$y = 0.1396\ln(x) + 5.1444$
		2025	$y = 0.1396\ln(x) + 5.2493$
		2050	$y = 0.1396\ln(x) + 5.5114$
		2100	$y = 0.1396\ln(x) + 6.0357$
Summer	RCP 2.6	2015	$y = 0.063\ln(x) + 4.8045$
		2025	$y = 0.063\ln(x) + 4.9033$
		2050	$y = 0.063\ln(x) + 5.1502$
		2100	$y = 0.063\ln(x) + 5.6441$

Table 10 Winter and summer RCP 8.5 logarithmic equation

Season	Scenario	Timescale	Logarithmic Equation
Winter	RCP 8.5	2015	$y = 0.1396\ln(x) + 5.1768$
		2025	$y = 0.1396\ln(x) + 5.4438$
		2050	$y = 0.1396\ln(x) + 6.111$
		2100	$y = 0.1396\ln(x) + 7.4456$
Summer	RCP 8.5	2015	$y = 0.063\ln(x) + 4.835$
		2025	$y = 0.063\ln(x) + 5.0865$
		2050	$y = 0.063\ln(x) + 5.7151$
		2100	$y = 0.063\ln(x) + 6.9722$

For more details regarding to the other RCP scenarios and their resultant sea level elevations see Appendix G

Before the simulation process could take place the datums of all data must be aligned to a single vertical referencing system. The two types of vertical data used are tidal gauge data and the CDEM file. The tidal gauge data uses a chart datum system for vertical referencing, while the CDEM file uses the mean sea level (MSL) which is also known as Canadian Geodetic Vertical Datum of 1928 (CGVD28). To properly align the data the tidal gauge data was shifted towards the CGVD28 datum level using a separation value. Separation values around Vancouver vary depending on location. Therefore an empirical analysis is done to determine which separation values could be considered to be an average. Once averaged, the separation value is subtracted from the sea level elevation values, aligning the data to the CGVD28 datum level. Figure 37 is an image of the available locations. The green dots represent separation values used, while the red dots are not included in the average. See Appendix H for details.
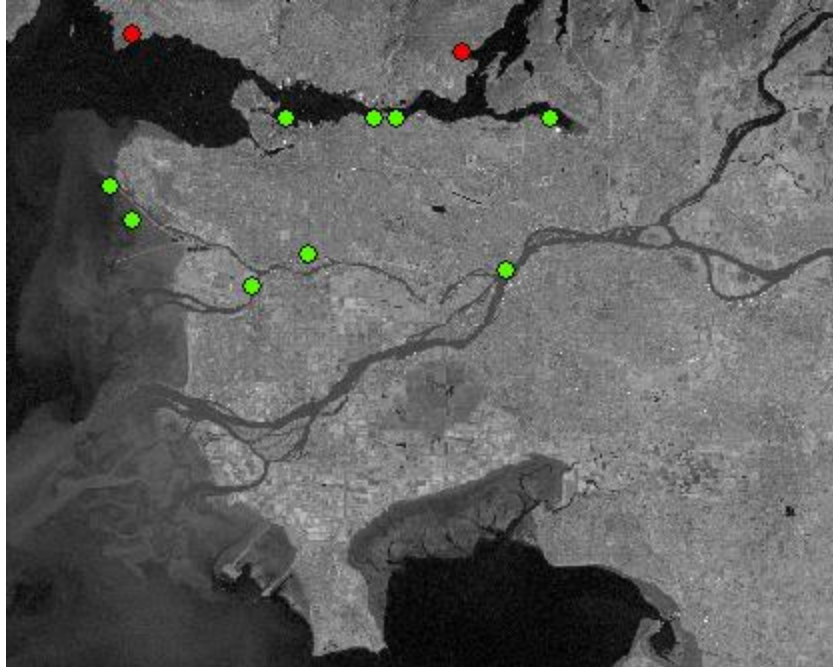
Figure 37 Locations of stations that carry separation values used in average. Green dots were included in average and red dots were omitted

4.3 Results

Method 1 Results: Deterministic Analysis

The inundation maps are created for every decade from 2014-2100 for RCP scenarios 2.6 and 8.5. To gain further insight into the effects of SLR time slices from 2014 and 2100 are compared to identify the areas at risk. Figures 38 and 39 are showing inundation maps comparing RCP 2.6 to RCP 8.5 scenarios, for years 2014 and 2100 respectively. Considering Figure 38 the areas at risk of future inundation can be easily located as well as the difference between the scenarios, as this is highlighted in purple.
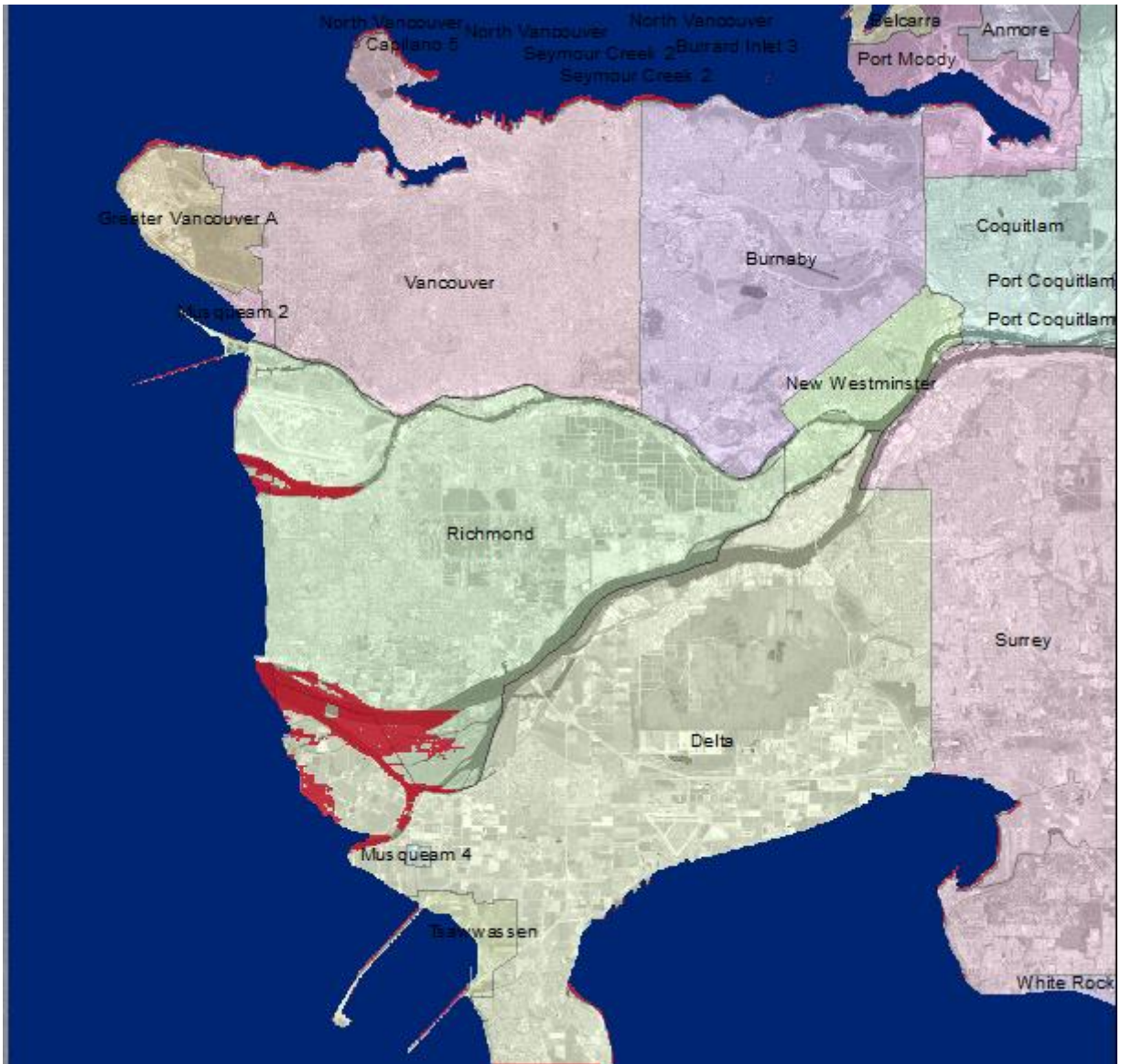
Figure 38 2050 inundation results for RCP 2.6 and RCP 8.5. Red represents RCP 2.6 and purple and red represents RCP 8.5
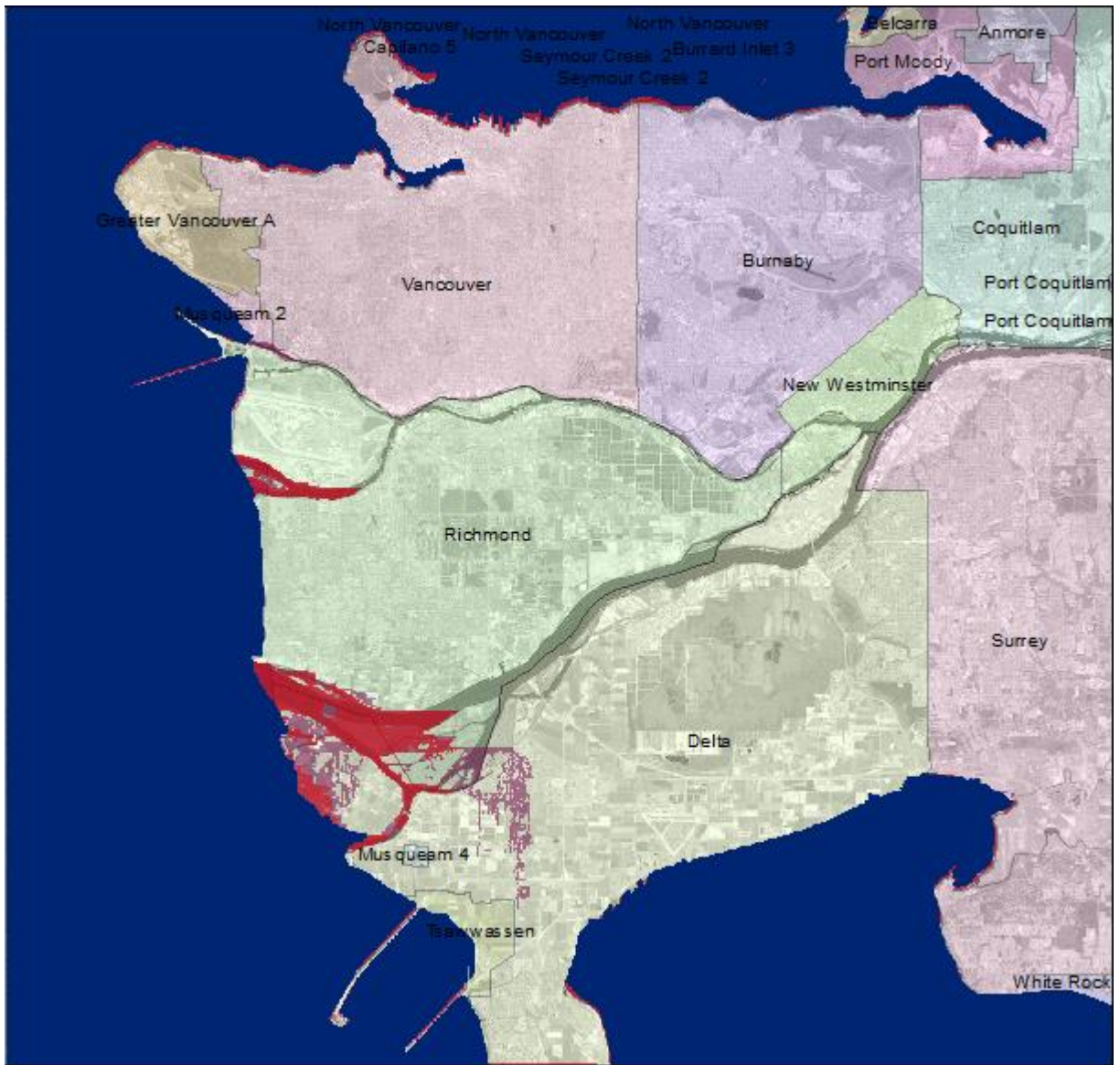
Figure 39 2100 inundation results for RCP 2.6 and RCP 8.5. Red represents RCP 2.6 and purple and red represents RCP 8.5.

When considering method one results, it is clear that SLR is a long term problem. This is evident from the comparison between Figure 38 to Figure 39. Looking at Figure 38 one can see that for both RCP scenarios, 2.6 and 8.5 there is no significant difference and little inundation. Comparing this to Figure 38 a difference is visible, as the outcome for RCP scenario 8.5 results in inundation of the lower lying delta region of Vancouver. Therefore the conclusion is that inundation of land only occurs for both RCP scenario 8.5 and 2.6 by 2100. For all inundation maps for RCP scenarios 2.6 and 8.5 for the years 2014, 2050 and 2100 see Appendix I.

Method 2 Results: Probabilistic Method

For the second method inundation maps are created for two time periods, 2025 and 2100. This is done in order to consider the short and long term effects of SLR and the associated hazard of storm surges. Maps are created for both, summer and winter seasons to capture the natural minimum and maximum cases, and again for both RCP scenario 2.6 and 8.5. All maps presented in Figures 40 – 43 show a 200 year return period event. The maps are layered so that the red represents summer and the red and purple represent winter.
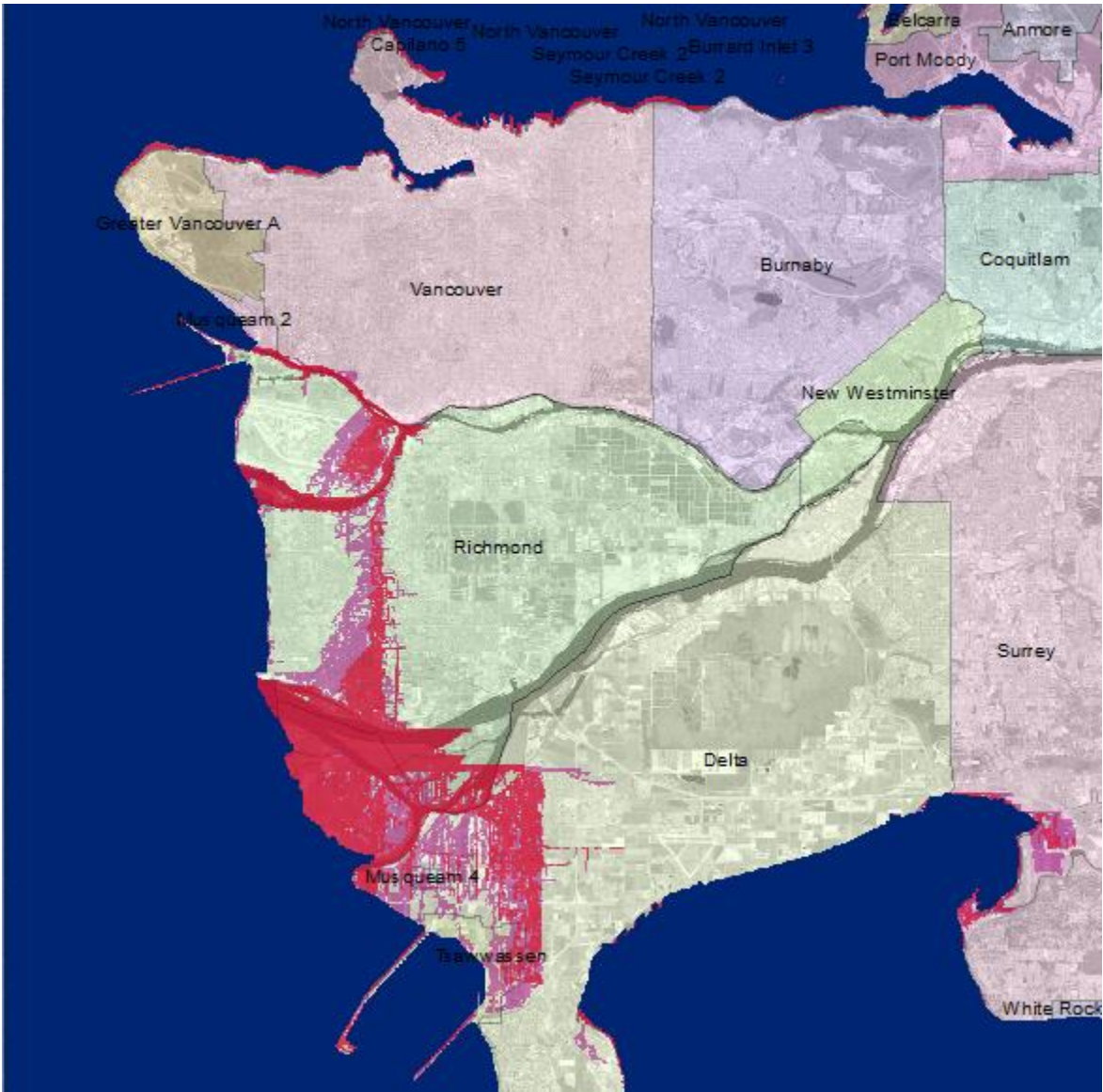
Figure 40 Inundation results for summer and winter seasons, RCP 2.6, 2025 - 200 years return period. Red represents summer and purple and red represents winter.
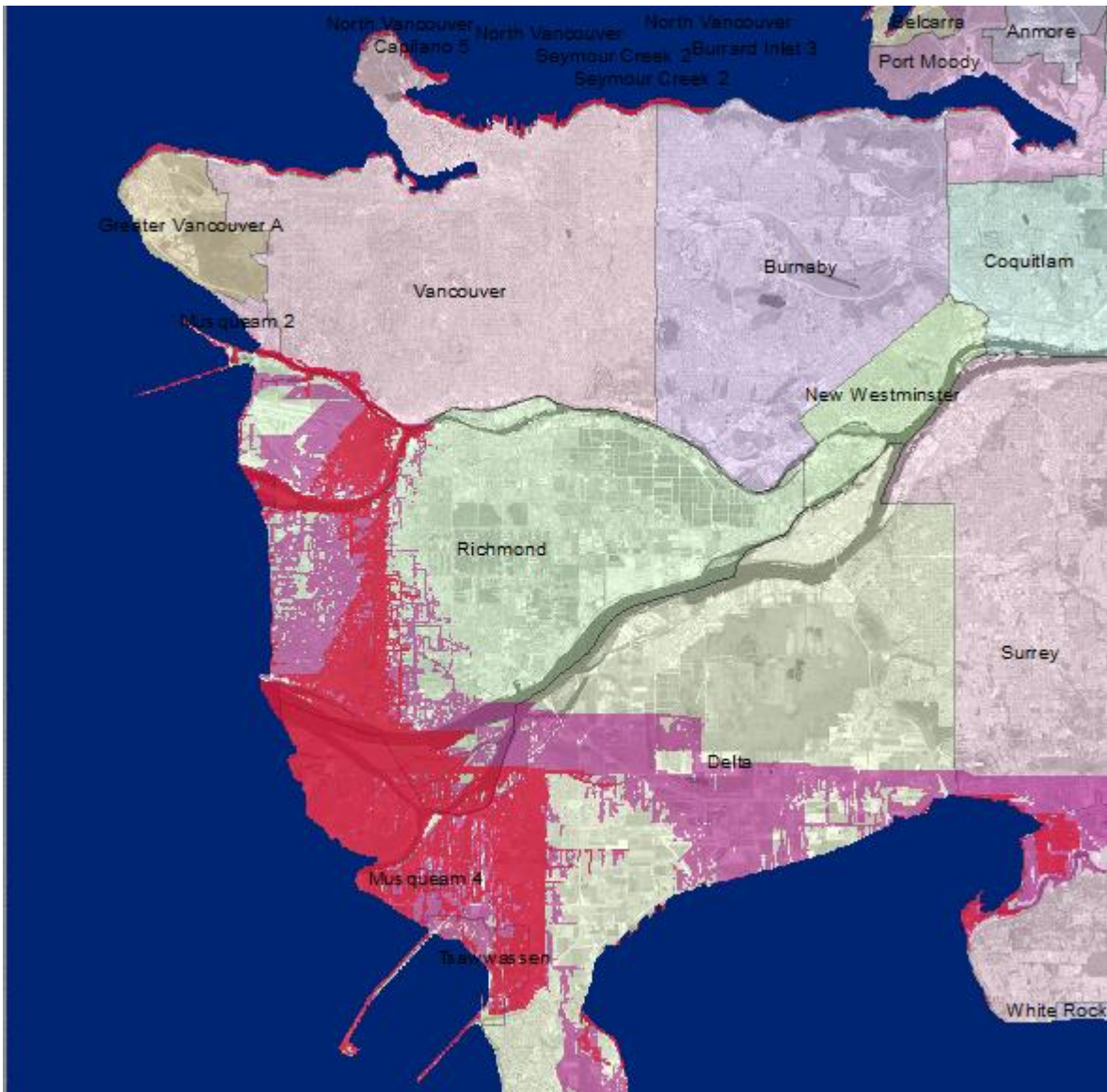
Figure 41 Inundation results for summer and winter seasons, RCP 2.6, 2100 - 200 years return period. Red represents summer and purple and red represents winter.
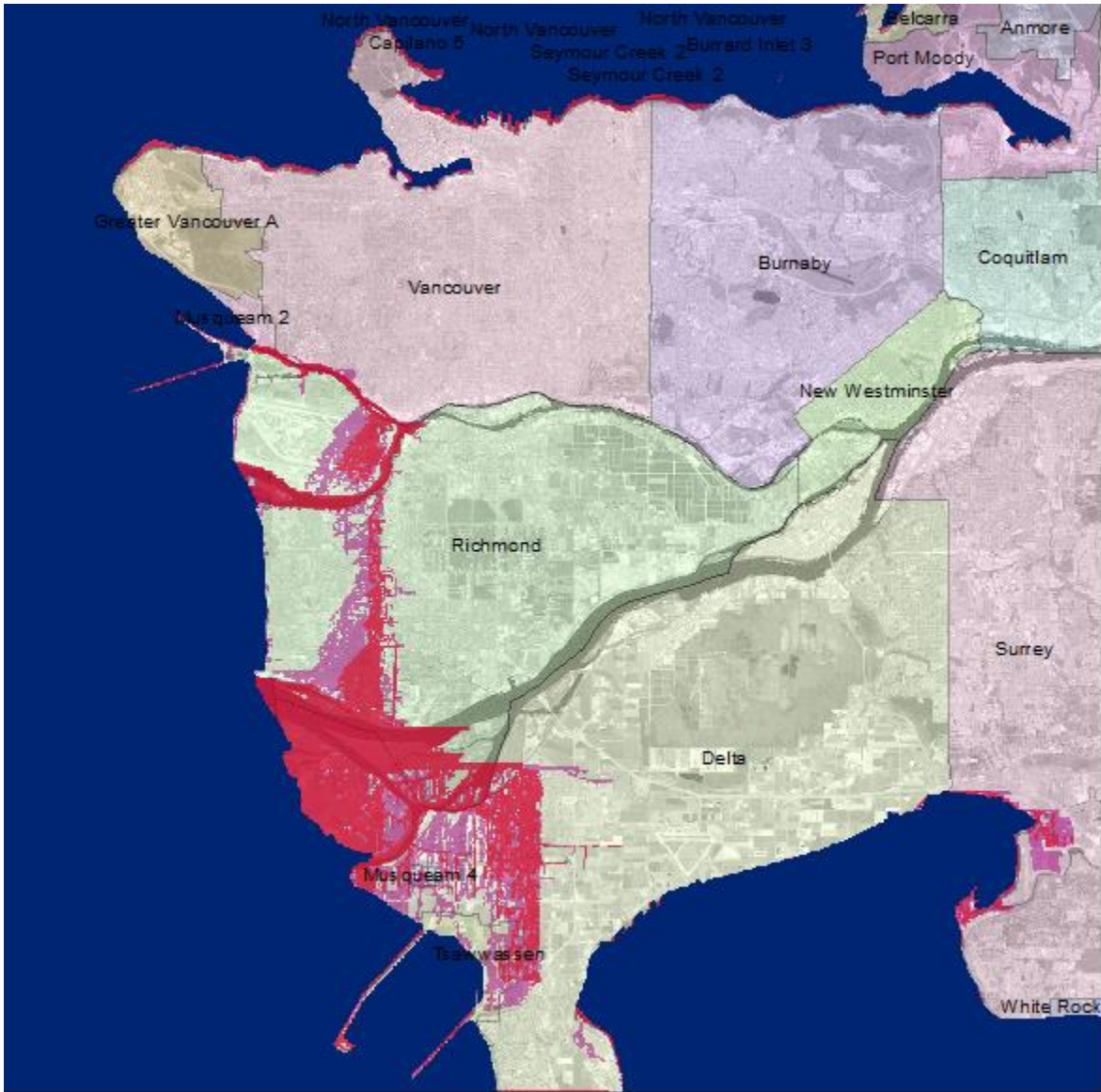
Figure 42 Inundation results for summer and winter seasons, RCP 8.5, 2025 - 200 years return period. Red represents summer and purple and red represents winter.
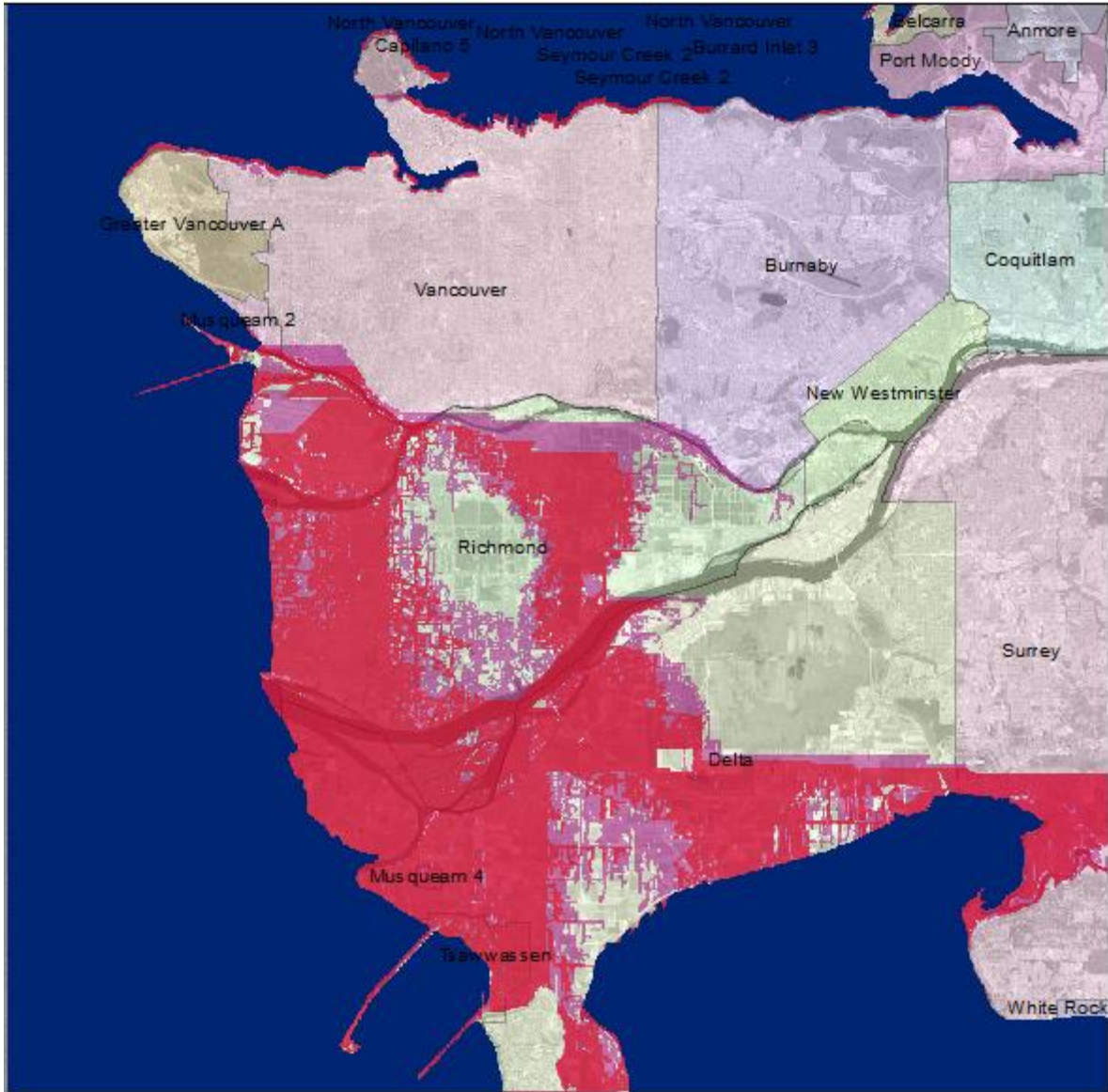
Figure 43 Inundation results for summer and winter seasons, RCP 8.5, 2100 - 200 years return period. Red represents summer and purple and red represents winter.

When considering probabilistic method results it is clear that Vancouver needs to consider the effects of extreme events. As expected more areas are being inundated during the winter season compared to the summer season. Comparing Figures 40 to 41 it is obvious that the risk of

inundation in the lower lying Delta region is increasing. Figures 40 and 42 are near identical meaning that according to RCP 2.6 and RCP 8.5 a 200 year event will lead to the same amount of land being inundated by the year 2025. Comparison of Figures 41 and 43 shows increase in the inundation of Richmond area for year 2100. When considering Figure 42 a linearity can be seen within the results, this area was deemed as a barrier where the water cannot pass. After a closer examination of the DEM file it was found that a ridge is the consequence of used interpolation technique.

For RCP 2.6 and 8.5 considering the deterministic method by 2050, there is little inundation in the Vancouver and Greater Vancouver area, this is illustrated by Figure 38. Comparing this to the probabilistic method for a 200 year event by the year 2025 there is a large amount of inundation in the Richmond area as well as the lower lying Delta region, illustrated by Figures 40 and 42. Figures 39, 41 and 43 are used to illustrate the effects of SLR by 2100, one can conclude that extreme events will cause more concern than the general rise of sea level. This is established by Figure 39, as it illustrates little inundation in the Delta region, while Figures 41 and 43 show large amounts of inundation in the Richmond and Delta region.

When comparing the deterministic method to the probabilistic method, the probabilistic method leads to worse inundation for all time scales and scenarios. The deterministic method allows one to gain an idea of the threat of SLR and the permanent inundation it causes. While the probabilistic method illustrates areas at risk of temporary inundation caused by extreme events. For all results see Appendix J.

6.0 Conclusion

Climate change is an issue that has serious socio-economic consequences for Canada. It affects many aspects of life, some of which include: international politics, economics, migration, human rights, development, trade, health and environment (Dokos 2008). It affects everyone one on a multitude of levels, and has the potential to change both the day-to-day actions of an individual, as well as one's life. A change in climate has the ability to enhance, or reduce the effect of water, wind and other disasters. This ability is the source of its power, as unforeseen extreme events, can be created within minutes.

SLR is an influential hazard created by climate change. When considering the threat of SLR the two main concerns are the steady rise of GMSL, and the increase in frequency and magnitude of all wave events. To gain insight into these processes two methods were implemented in this research, a deterministic and a probabilistic analysis methods. The deterministic analysis method was able to illustrate the effects of SLR for four different emission scenarios. More focus is given in this research to the extreme RCP scenarios 2.6 and 8.5 as a potential source of better understanding of effects of SLR. The results of the implementation of this method to SLR impacts on Vancouver is showing no inundation of land until 2100. The implementation of the probabilistic method identifies areas of inundation created by extreme event. The area of Vancouver often experiences events known as king tide events, which are created by astronomical tidal patterns. These events are considered in the probabilistic analysis as the BM method of sampling data captured the maximum values between 1943 and 2013. Comparison between these methods clearly shows that the probabilistic method leads to more significant SLR impacts. This is expected, as when the sea levels rise the moorland gets inundated. The inundation maps developed in this research can serve as the basis for definition of the risk associated with SLR. The identified areas of inundation as the locations of hazard can be combined with exposure in order to assess the risk.

The Vancouver coastline is at risk of future inundation due to the sea level rise and extreme events, like storm surges. Considering the time scale, SLR is a long term problem. However to avoid disasters in the future these events must be considered now in planning adaptation and mitigation activities in the region. The final results of the presented research can aid the local

government planners and decision makers in making policy decisions that will minimize the potential negative impacts of sea level rise in the future.

For future work it is recommended that a more recent and detailed elevation data is used. The CDEM file used in this work was created between the years 1981-1990 and has an accuracy of meters. Since SLR acts on the scale of millimeters the detailed elevation data are needed. Gaining this kind of accuracy is difficult, however with the use of LIDAR data a high resolution maps can be generated. It is also important that the data be as recent as possible to include any new protection infrastructure (dikes or protective structures) that can change the movement of water A use of a hydrodynamic model to capture the movement of water when determining the effects of extreme events will be beneficial.

References

Aral, M.M., Guan, J., Chang, B. (2012) Dynamic System Model to Predict Global Sea-Level   Rise and Temperature Change. *Journal of Hydrologic Engineering*

Arns, A., Wahl, T., Haigh, I.D., Jensen, J., and Pattiaratchi, C. (2013) Estimating extreme water level probabilities: A comparison of the direct methods and recommendations for best practice. *Coastal Engineering*, 81 (2013) 51–66

Ausenco Sandwell.(2011) Climate Change Adaption Guidelines for Sea Dikes and Coastal Flood Hazard Land Use. *BC Ministry of Environment*

Chruch, J., White, N., Hunter, J., McInnes, K., Cowell, P., O'Farrell, S. (2008) Sea-level Rise: Transitions: Transitioning to Resilient Cities. *CSIRO Publishing, Australia*

Church, J.A., Clark, P.U., Cazenave, A., Gregory, J.M., Jevrejeva, S., Levermann, A., Merrifield, M.A., Milne, G.A., Nerem, R.S., Nunn, P.D., Payne, A.J., Pfeffer, W.T., Stammer, D. and Unnikrishnan. A.S. (2013) Sea Level Change. *In: Climate Change 2013: The Physical Science Basis. Contribution of Working Group I to the Fifth Assessment Report of the Intergovernmental Panel on Climate Change* [Stocker, T.F., D. Qin, G.-K. Plattner, M. Tignor, S.K. Allen, J. Boschung, A. Nauels, Y. Xia, V. Bex and P.M. Midgley (eds.)]. Cambridge University Press, Cambridge, United Kingdom and New York, NY, USA.

Codiga, D.L. (2011) Unified Tidal Analysis and Prediction Using the UTide Matlab Functions. *Technical Report 2011- 01. Graduate School of Oceanography, University of Rhode Island, Narragansett, RI*. 59pp. ftp://www.po.gso.uri.edu/pub/downloads/codiga/pubs/2011Codiga-UTide-Report.pdf / [Accessed 17 June 2013]

Coles, S.(2001) An Introduction to Statistical Modeling of Extreme Values. *Springer Series in Statistics*. ISBN (print) 1-85233-459-2

Delta Committee. (2008) Working Together with Water - A Living Land Builds for its Future. http://www.deltacommissie.com : Delta Committee, 2008. pp. 134*.

Denny, M., Paine, R. (1998) Celestial Mechanics, Sea-Level Changes, and Intertidal Ecology. *Biological Bulletin*, Vol. 194, No. 2 (Apr., 1998), pp. 108-115

Dixon, M.J., Tawn, J.A.(1994) Extreme sea-levels at the UK A-class sites: site-by-site analyses. *Proudman Oceanographic Laboratory Internal Document* No. 65

Dokos, Thanos.(2008) Climate Change: Addressing the Impact. *Hellenic Foundation for European and Foreign Policy (ELIAMEP)*

Eggleston, J., and Pope, J.(2013) Land Subsidence and Relative Sea-Level Rise in the Southern Chesapeake Bay Region. *U.S. Geological Survey Circular 1392*, 30 p., http://dx.doi.org/10.3133/cir1392.

ESRI (2011) ArcGIS Desktop: Release 10. *Redlands, CA: Environmental Systems Research Institutex*

Grossman, W.D., and Eberhardt, S.(1992) Geographical Information Systems and Dynamic Modelling. *Annals of Regional Science 26: 53-66.*

Harford, D. (2008) Climate Change Adaptation: Planning for BC. *Pacific Institute for Climate Solutions, University of Victoria*.

Heathfield, D.K., Walker, I. J., and Atkinson, D.E.(2012) Erosive water level regime and climatic variability forcing of beach–dune systems on south-western Vancouver Island, British Columbia, Canada. *Earth Surface Processes and Landforms*

Li, X., Rowley, R..,Kosetlnick, J., Braaten, D., Meisel, J., Hulbutta K.(2009) GIS Analysis of Global Impacts from Sea Level Rise. *Photogrammetric Engineering & Remote Sensing.*

NASA. (2012) Is sea level rising? Do we have to worry about it?. *Gordon Space Flight Center NASA*.

Nicholls, R.J. and Small, C. (2002) Improved Estimates of Coastal Population Exposure to Hazards Released. *Eos, Transactions American Geophysical Union,* Volume 83, Issue 28, pages 301–305

MATLAB 7.1.2 (2011). The MathWorks, Inc., Natick, Massachusetts, United States.

Murdukhayeva, A., August, P., Bradley, M., LaBash, C. and Shaw, N. (2013) Assessment of Inundation Risk from Sea Level Rise and Storm Surge in Notheastern Coastal National Parks. Journal of Coastal Research. *Coconut Creek, Florida*

PostNote 363 (2010) Sea Level Rise. *Houses of Parliament: Parliamentary Office of Science and Technology 7 Millbank, London*

Python Software Foundation. (2014) Python Language Reference, version 3.4. Available at http://www.python.org

Rakhecha, P.R., and Singh, V.P.(2009) Applied Hydrometerology. *Springer*. ISBN (ebook) 978-1-4020-9844-4

Ruth, M. and Pieper, F.(1993) Modeling spatial dynamics of sea-level rise in a coastal area. *System Dynamics Review.*

Sahin, O. and Mohamed, S. (2010) Sea Level Rise and Adaptation Responses for Coastal Construction: A Spatial – Temporal Decision Making Tool. *Advancing and Integrating Construction Education , Research & Practice.*

Schubert, R., Schellnhuber, H.-J., Buchmann, N., Epiney, A., Grießhammer, R., Kulessa, M., Messner, D., Rahmstorf, S., Schmid, J. (2006) The Future Oceans – Warming Up, Rising High, Turning Sour. *German Advisory Council on Global Change (WBGU)*

Seltman, H.J. (2009) Experimental Design and Analysis. http://www.stat.cmu.edu/~hseltman/309/Book/[Accessed 28 February 2014]

Strauss, B., Tebaldi, C., Kulp, S.(2014) North Carolina and the Surging Sea: A vulnerability assessment with projections for sea level rise and coastal flood risk. *Climate Central*

The Arlington Group Planning and Architecture Inc., EBA, a Tetra Tech Company, DE Jardine Consulting, Sustainability Solutions Group. (2013) Sea Level Rise Adaptation Primer A Toolkit To Build Adaptive Capacity On Canada's South Coasts. *BC Ministry of Environment*

The Comet Program. (2012) Climate Change and Sea Level Rise*. University Corporation for Atmospheric Research.*

The World Bank. (2012) Turn Down the Heat: Why a 4°C Warmer World Must be Avoided. *Potsdam Institute for Climate Impact Research and Climate Analytics*.

Teetor, P., 2011. R Cookbook. *O'Reilly Media*. ISBN (print) 978-0-596-80915-7

University of Arizona, 2013. *GEOS 585A Notes_7 – Detrending*. http://www.ltrr.arizona.edu/~dmeko/notes_7.pdf [Accessed 22 January 2014]

University of Colorado, 2011. What is the definition of global mean sea level (GMSL) and its rate?. http://sealevel.colorado.edu/content/what-definition-global-mean-sea-level-gmsl-and-its-rate [Accessed 11 September 2014]

Wayne, G.P. (2013) The Beginner's Guide to Representative Concentration Pathways. *Skeptical Science*

Appendices

Appendix A: Python code for cell classification

import arcpy

import numpy

Change rasterFile to array; This is done for both elevation and cover matrices

Elevation_Matrix = arcpy.RasterToNumPyArray("C:/Users/Owner/Documents/ArcGIS/Default.gdb/Float_raster3_Resample")

Cover_Matrix = arcpy.RasterToNumPyArray("C:\Users\Owner\Documents\ArcGIS\Default.gdb\Lookup_raste5_Clip4")

Return the rows, columns for the elevation matrix

rows, cols = Elevation_Matrix.shape

print rows

print cols

Return the rows, columns for the cover matrix

rows2, cols2 = Cover_Matrix.shape

print rows2

print cols2

Defines the sea level elevation depending on the year

Sea_Level=4.695993994

##
################### Corner Code #########################
##

Static Referencing: floods corner cells conditional to the surrounding cells being water and the elevation being less than the sea level

#Top left corner

if Cover_Matrix[0][0]==0 and (Cover_Matrix[1][0]==2 or Cover_Matrix[1][1]==2 or Cover_Matrix[0][1]==2) and Elevation_Matrix[0][0]<Sea_Level :

 Cover_Matrix[0][0]=2

#Top right corner

if Cover_Matrix[0][7685]==0 and (Cover_Matrix[1][7685]==2 or Cover_Matrix[1][7684]==2 or Cover_Matrix[0][7684]==2) and Elevation_Matrix[0][7685]<Sea_Level :

 Cover_Matrix[0][7685]=2

#Bottom left corner

if Cover_Matrix[7073][0]==0 and (Cover_Matrix[7072][0]==2 or Cover_Matrix[7073][1]==2 or Cover_Matrix[7072][1]==2) and Elevation_Matrix[7073][0]<Sea_Level :

 Cover_Matrix[7073][0]=2

#Bottom right corner

if Cover_Matrix[7073][7685]==0 and (Cover_Matrix[7073][7684]==2 or Cover_Matrix[7072][7684]==2 or Cover_Matrix[7072][7685]==2) and Elevation_Matrix[7073][7685]<Sea_Level :

 Cover_Matrix[7073][7685]=2

###

#################### Border Code ############################

###

#Top Border

for colNum in xrange(1,7684):

      if Cover_Matrix[0][colNum]==0 and \

      (Cover_Matrix[0][colNum-1]==2 or Cover_Matrix[0][colNum+1]==2 or \

       Cover_Matrix[1][colNum-1]==2 or Cover_Matrix[1][colNum]==2 or Cover_Matrix[1][colNum+1]==2) \

       and Elevation_Matrix[0][colNum]<Sea_Level:

       Cover_Matrix[0][colNum]=2

```python
#Bottom Border

for colNum in xrange(1,7684):

    if Cover_Matrix[7073][colNum]==0 and \

    (Cover_Matrix[7073][colNum-1]==2 or Cover_Matrix[7073][colNum+1]==2 or \

    Cover_Matrix[7072][colNum-1]==2 or Cover_Matrix[7072][colNum]==2 or Cover_Matrix[7072][colNum+1]==2) \

    and Elevation_Matrix[7073][colNum]<Sea_Level:

    Cover_Matrix[7073][colNum]=2

#Left Border

for rowNum in xrange(1,7072):

    if Cover_Matrix[rowNum][0]==0 and \

    (Cover_Matrix[rowNum-1][0]==2 or Cover_Matrix[rowNum-1][1]==2 or \

    Cover_Matrix[rowNum][1]==2 or Cover_Matrix[rowNum+1][0]==2 or Cover_Matrix[rowNum+1][1]==2) \

    and Elevation_Matrix[rowNum][0]<Sea_Level:

    Cover_Matrix[rowNum][0]=2




#Right Border

for rowNum in xrange(1,7072):

    if Cover_Matrix[rowNum][7685]==0 and \

    (Cover_Matrix[rowNum-1][7685]==2 or Cover_Matrix[rowNum-1][7684]==2 or \

    Cover_Matrix[rowNum][7685]==2 or Cover_Matrix[rowNum+1][7685]==2 or Cover_Matrix[rowNum+1][7684]==2) \

    and Elevation_Matrix[rowNum][7685]<Sea_Level:

    Cover_Matrix[rowNum][7685]=2
```

```
###################################################################
#################### Internal Code ###########################
###################################################################


for rowNum in xrange(1,7072):

    for colNum in xrange(1,7684):

        if Cover_Matrix[rowNum][colNum]==0 and \

        (Cover_Matrix[rowNum][colNum-1]==2 or Cover_Matrix[rowNum][colNum+1]==2 or \

            Cover_Matrix[rowNum+1][colNum-1]==2 or Cover_Matrix[rowNum+1][colNum]==2 or
Cover_Matrix[rowNum+1][colNum+1]==2 or \

            Cover_Matrix[rowNum-1][colNum-1]==2 or Cover_Matrix[rowNum-1][colNum]==2 or
Cover_Matrix[rowNum-1][colNum+1]==2) \

        and Elevation_Matrix[rowNum][colNum]<Sea_Level:

            Cover_Matrix[rowNum][colNum]=2


print Cover_Matrix
###################################################################
#################### Save New Raster#######################
###################################################################
descData=arcpy.Describe("C:/Users/Owner/Documents/ArcGIS/Default.gdb/Float_raster3_Resample")

cellSize=descData.meanCellHeight

extent=descData.Extent

spatialReference=descData.spatialReference

pnt=arcpy.Point(extent.XMin,extent.YMin)

Cover_Raster = arcpy.NumPyArrayToRaster(Cover_Matrix,pnt, cellSize,cellSize)

arcpy.DefineProjection_management(Cover_Raster,spatialReference)

Cover_Raster.save("C:/Users/Owner/Documents/ArcGIS/Default.gdb/V2_Summer_85_2100_200")
```

Appendix B: Accuracy and validity Index for CDEM File

Accuracy Index

Validity Date Index

Canadian Digital Elevation Model (CDEM)
Validity Date

Legend
1945
1946 - 1950
1951 - 1960
1961 - 1970
1971 - 1980
1981 - 1990
1991 - 2000
2001 - 2010
2011
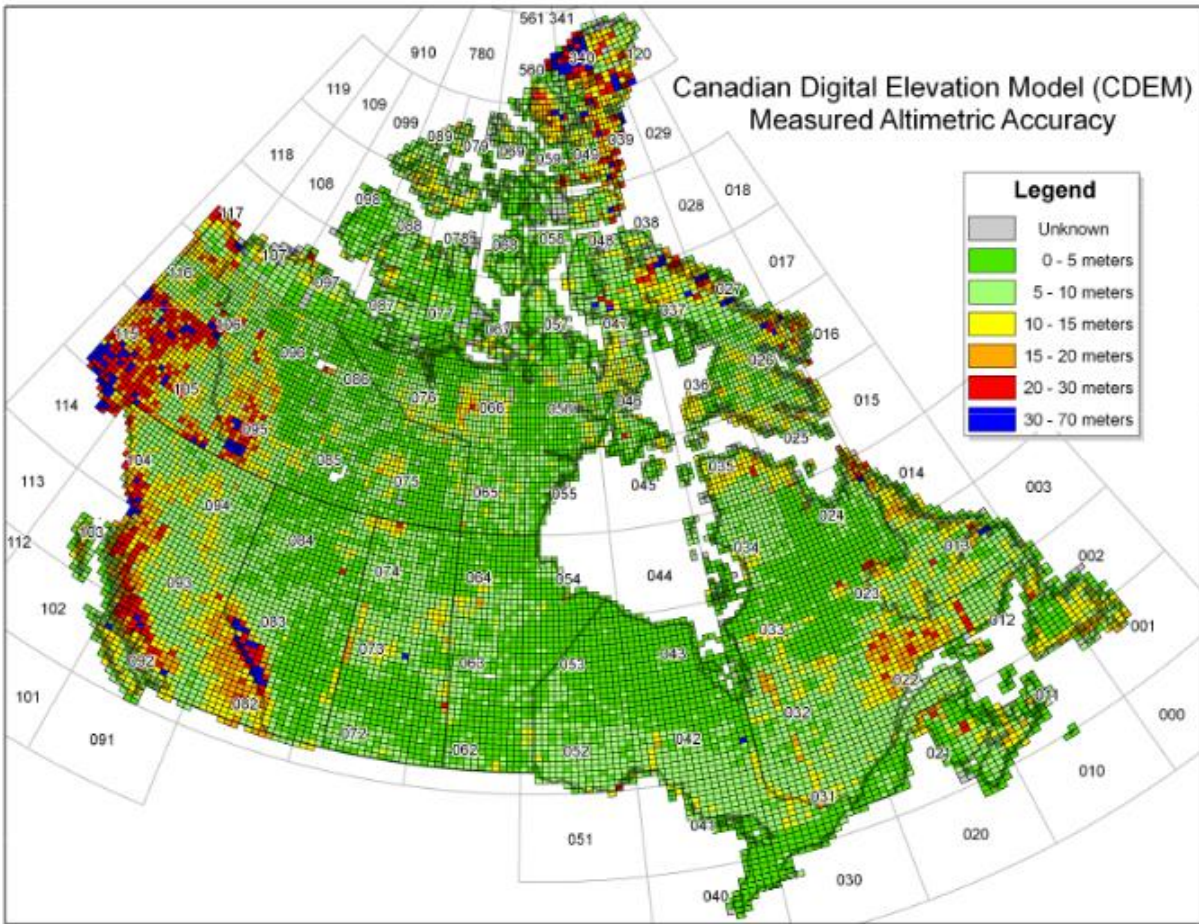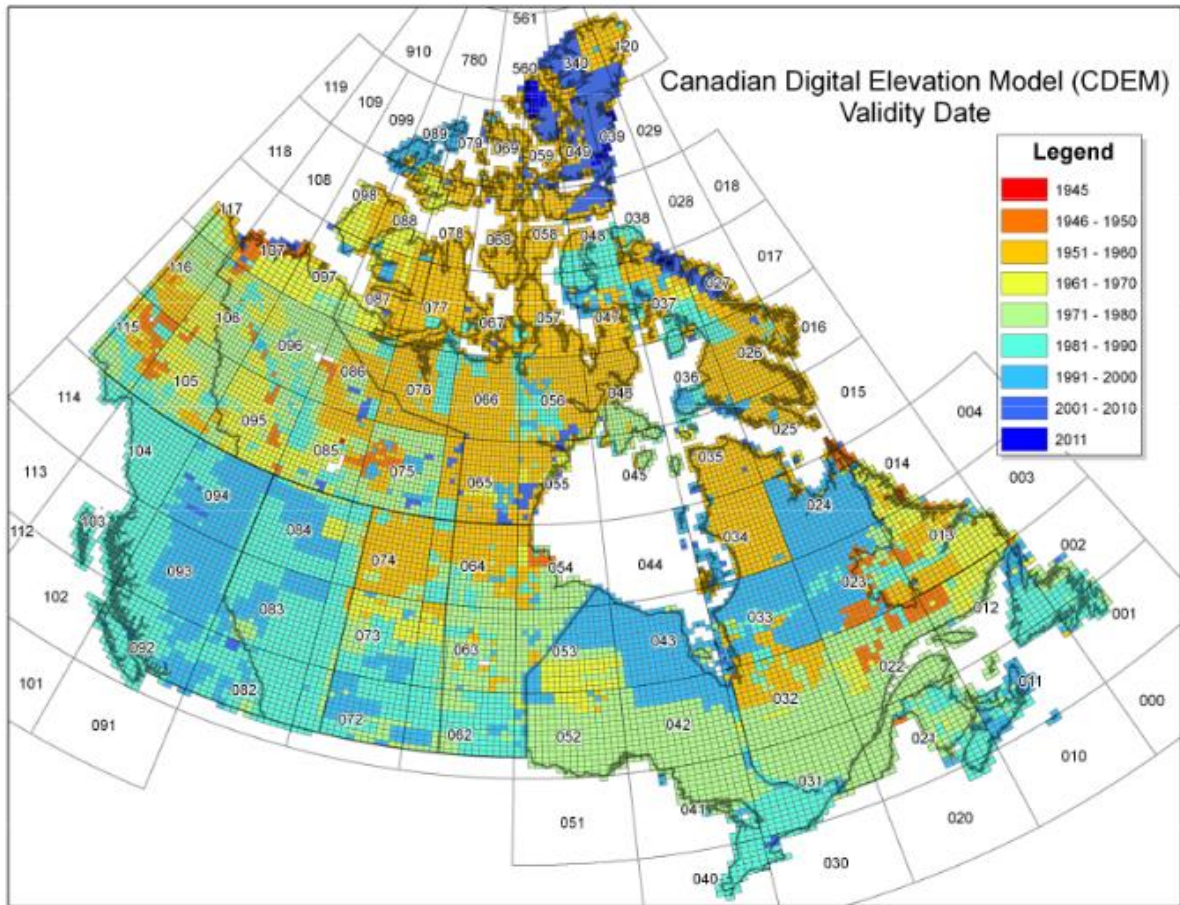
Appendix C: U_Tide input details

Property	Description	Included
Summary of Desired Options		
NoTrend	Used to remove linear trend	🟩
PreFilt	Used to correct for pre-filtering	🟥
NodsatNone	Used to omit nodal corrections	🟩
GwchNone	Used to omit astronomical arguments (not referenced to Greenwich)	🟩
Infer	Used to infer constitutents	🟥
InferAprx	Compliments	🟥
Rmin	Use "1" is record length is long	🟥
OLS	Ordinary Least Squares Method	🟥
TunRdn	Willl run with default=1, MUST re-evaluate after first run	🟥
LinCI	Will use default Monte Carlo technique	🟥
White	Will resort to the colour residual spectra	🟥
Nrlzn	Will use default 200; Must re-evaluate after first run	🟥
LSFrqOSmp	Will use default; Must re-evaluate after first run	🟥
DiagnMinSNR	Will use default	🟥
DiagnPlots	Plots data	🟩
OrderCnstit	Re-orders constitutents	🟥
RunTimeDisp	Displays time; Will use default	🟥

🟩 Include

🟥 Omit

Appendix D: Excel macro code for extracting maximum values

When R=1 Only one maximum value is returned **for each season**

- **Excel Equation: Finds the maximum amongst the 3 seasons**
    - =MAX(
      MAX(IF(TEXT(F2,"mmyyyy")=TEXT($A$2:$A$611659,"mmyyyy"),$B$2:$B$61165
      9)) **(Month1)**
      MAX(IF(TEXT(F3,"mmyyyy")=TEXT($A$2:$A$611659,"mmyyyy"),$B$2:$B$61165
      9)) **(Month2)**

MAX(IF(TEXT(F13,"mmyyyy")=TEXT($A$2:$A$611659,"mmyyyy"),$B$2:$B$6116
59))) **(Month3)**

- o **Marco: Used to find the maximum values for 1 season at a time. Filters through the arrays and finds the maximum value depending on the month.**

    y = **44**

    For x = **462 To 798**

       Range("G" & y).Select

       Selection.FormulaArray = _

          "=MAX(MAX(IF(TEXT(R[& **x** &]C[**3**],""mmyyyy"")=TEXT(R2C1:R611659C1,""mmyyyy""),R2C2:R611659C2)),MAX(IF(TEXT(R[& (**x+1**) &]C[**3**],""mmyyyy"") = TEXT(R2C1:R611659C1,""mmyyyy""),R2C2:R611659C2)),MAX(IF(TEXT(R[& (**x+11**) &]C[-**3**],""mmyyyy"")=TEXT(R2C1:R611659C1,""mmyyyy""),R2C2:R611659C2)))"

       y = y + 1

       Next x

       End Sub

When R > 1

- • **Excel Equation: Finds the Second highest value based on both conditions**
    - ▪ **Condition 1: Month – Year Comparison**
    - ▪ **Condition 2: Must be 24 hours from first value. Done taking the absolute difference of the Excel Dates and ensuring its greater than 24hours**
    - ▪

=MAX(IF((TEXT(F2,"mmyyyy")=TEXT($A$2:$A$616070,"mmyyyy"))*(ABS(I2-
$D$2:$D$616070)>0.95833333333394),$B$2:$B$616070))

The final macro code for R=2-6 was as follows:

    Sub fillout7()

    ' fillout7 Macro

    x = 8

    Z = 0

    For y = 2 To 72

    Range("BD" & y).Select

```
        Selection.Formula = "=MAX(MAX(IF((TEXT(R[" & x & "]C[-
50],""mmyyyy"")=TEXT(R2C1:R616070C1,""mmyyyy""))*" & _

            "(ABS(R[" & Z & "]C[-41]-R2C4:R616070C4)>0.95833333333394)*" & _

            "(ABS(R[" & Z & "]C[-33]-R2C4:R616070C4)>0.95833333333394)*" & _

            "(ABS(R[" & Z & "]C[-25]-R2C4:R616070C4)>0.95833333333394)*" & _

            "(ABS(R[" & Z & "]C[-17]-R2C4:R616070C4)>0.95833333333394)*" & _

            "(ABS(R[" & Z & "]C[-9]-R2C4:R616070C4)>0.95833333333394)" & _

            ",R2C2:R616070C2)), " & "MAX(IF((TEXT(R[" & (x + 1) & "]C[-
50],""mmyyyy"")=TEXT(R2C1:R616070C1,""mmyyyy""))*" & _

            "(ABS(R[" & Z & "]C[-41]-R2C4:R616070C4)>0.95833333333394)*" & _

            "(ABS(R[" & Z & "]C[-33]-R2C4:R616070C4)>0.95833333333394)*" & _

            "(ABS(R[" & Z & "]C[-25]-R2C4:R616070C4)>0.95833333333394)*" & _

            "(ABS(R[" & Z & "]C[-17]-R2C4:R616070C4)>0.95833333333394)*" & _

            "(ABS(R[" & Z & "]C[-9]-R2C4:R616070C4)>0.95833333333394)" & _

            ",R2C2:R616070C2))," & "MAX(IF((TEXT(R[" & (x + 2) & "]C[-
50],""mmyyyy"")=TEXT(R2C1:R616070C1,""mmyyyy""))*" & _

            "(ABS(R[" & Z & "]C[-41]-R2C4:R616070C4)>0.9533333333394)*" & _

            "(ABS(R[" & Z & "]C[-33]-R2C4:R616070C4)>0.95833333333394)*" & _

            "(ABS(R[" & Z & "]C[-25]-R2C4:R616070C4)>0.95833333333394)*" & _

            "(ABS(R[" & Z & "]C[-17]-R2C4:R616070C4)>0.95833333333394)*" & _

            "(ABS(R[" & Z & "]C[-9]-R2C4:R616070C4)>0.9533333333394)" & _

            ",R2C2:R616070C2)))"

    x = x + 11

    Next y

    End Sub
```

This was completed by adding the formula through the macro, then manually entering the formula (Control + shift + enter) the formula into an FormulaArray The macro would not run if the macro contained the FormulaArray function because the function has a limit on the number of characters

The logic of the equation allowed for the previous r=x value to be ignored as well as any other value within a 24 hour time span. This was created to differentiate the events, it is thought that if the same event occurred within under a 24 hour time span event was only 1 event. Therefore the 24 hour time span was set to be the determining factor to differentiate events.

Appendix E: Matlab Code for maximum likelihood estimation

```
%This code is used to import in the maxima data per block(year) and perform

%a Maximum Likelihood Estimation to gain the following parameters

%paramEsts:

%   Shape parameter

%   Scale parameter

%   Location parameter

%paramCIs:

% 95% confidence intervals

%Imports the maxima data

x1 =xlsread('C:\Users\Nick\Documents\Graduate Work\Research
Project\Work\Storm Surge\Estimating Extreme Water Level
Prob\Block_Maxima_Method\Block_Maxima_Method_C_Return_Period_Graphs.xlsx',4
,'G2:G72');

%Performs MLE on the maxima data

[paramEsts1,paramCIs1] = gevfit(x1);

kMLE1 = paramEsts1(1) % Shape parameter

sigmaMLE1 = paramEsts1(2) % Scale parameter

muMLE1 = paramEsts1(3) % Location parameter


 % 95% confidence intervals

kCI1 = paramCIs1(:,1)

sigmaCI1 = paramCIs1(:,2)

muCI1 = paramCIs1(:,3)


x2 =xlsread('C:\Users\Nick\Documents\Graduate Work\Research
Project\Work\Storm Surge\Estimating Extreme Water Level
Prob\Block_Maxima_Method\Block_Maxima_Method_C_Return_Period_Graphs.xlsx',4
,'J2:J143');


%Performs MLE on the maxima data

[paramEsts2,paramCIs2] = gevfit(x2);

kMLE2 = paramEsts2(1) % Shape parameter

sigmaMLE2 = paramEsts2(2) % Scale parameter

muMLE2 = paramEsts2(3) % Location parameter
```

```matlab
% 95% confidence intervals

kCI2 = paramCIs2(:,1)

sigmaCI2 = paramCIs2(:,2)

muCI2 = paramCIs2(:,3)


x3 =xlsread('C:\Users\Nick\Documents\Graduate Work\Research
Project\Work\Storm Surge\Estimating Extreme Water Level
Prob\Block_Maxima_Method\Block_Maxima_Method_C_Return_Period_Graphs.xlsx',4
,'M2:M214');


%Performs MLE on the maxima data

[paramEsts3,paramCIs3] = gevfit(x3);

kMLE3 = paramEsts3(1) % Shape parameter

sigmaMLE3 = paramEsts3(2) % Scale parameter

muMLE3 = paramEsts3(3) % Location parameter



% 95% confidence intervals

kCI3 = paramCIs3(:,1)

sigmaCI3 = paramCIs3(:,2)

muCI3 = paramCIs3(:,3)


x4 =xlsread('C:\Users\Nick\Documents\Graduate Work\Research
Project\Work\Storm Surge\Estimating Extreme Water Level
Prob\Block_Maxima_Method\Block_Maxima_Method_C_Return_Period_Graphs.xlsx',4
,'P2:P285');


%Performs MLE on the maxima data

[paramEsts4,paramCIs4] = gevfit(x4);

kMLE4 = paramEsts4(1) % Shape parameter

sigmaMLE4 = paramEsts4(2) % Scale parameter

muMLE4 = paramEsts4(3) % Location parameter
```

```matlab
% 95% confidence intervals

kCI4 = paramCIs4(:,1)

sigmaCI4 = paramCIs4(:,2)

muCI4 = paramCIs4(:,3)



x5 =xlsread('C:\Users\Nick\Documents\Graduate Work\Research
Project\Work\Storm Surge\Estimating Extreme Water Level
Prob\Block_Maxima_Method\Block_Maxima_Method_C_Return_Period_Graphs.xlsx',4
,'S2:S356');



%Performs MLE on the maxima data

[paramEsts5,paramCIs5] = gevfit(x5);

kMLE5 = paramEsts5(1) % Shape parameter

sigmaMLE5 = paramEsts5(2) % Scale parameter

muMLE5 = paramEsts5(3) % Location parameter



% 95% confidence intervals

kCI5 = paramCIs5(:,1)

sigmaCI5 = paramCIs5(:,2)

muCI5 = paramCIs5(:,3)



x6 =xlsread('C:\Users\Nick\Documents\Graduate Work\Research
Project\Work\Storm Surge\Estimating Extreme Water Level
Prob\Block_Maxima_Method\Block_Maxima_Method_C_Return_Period_Graphs.xlsx',4
,'V2:V427');



%Performs MLE on the maxima data

[paramEsts6,paramCIs6] = gevfit(x6);

kMLE6 = paramEsts6(1) % Shape parameter

sigmaMLE6 = paramEsts6(2) % Scale parameter

muMLE6 = paramEsts6(3) % Location parameter
```
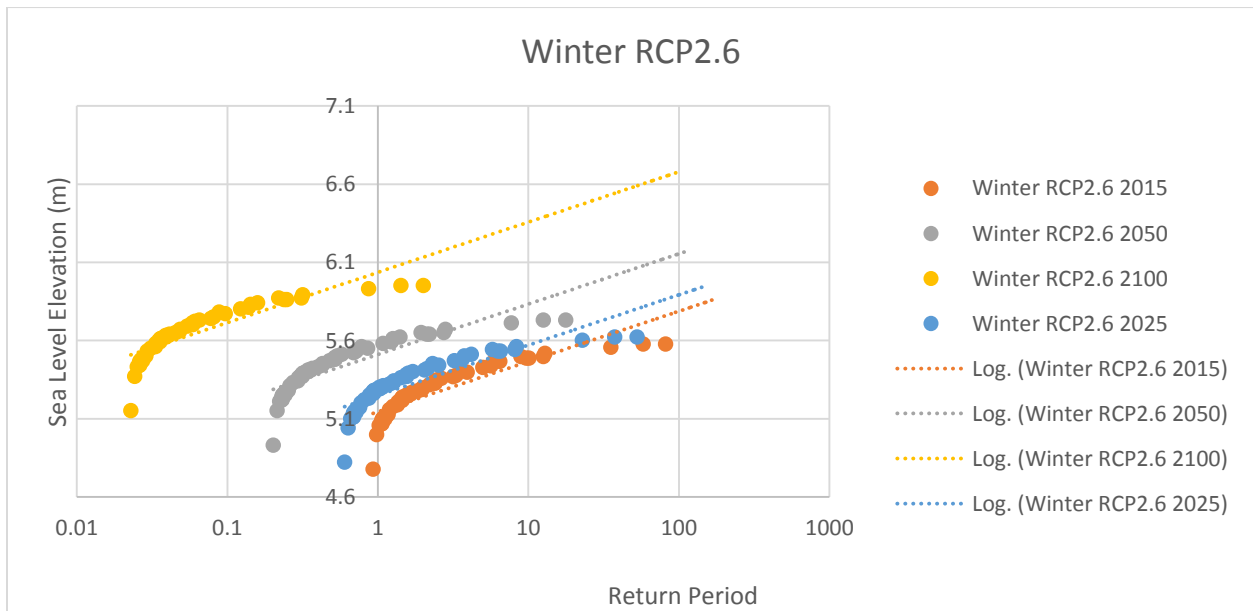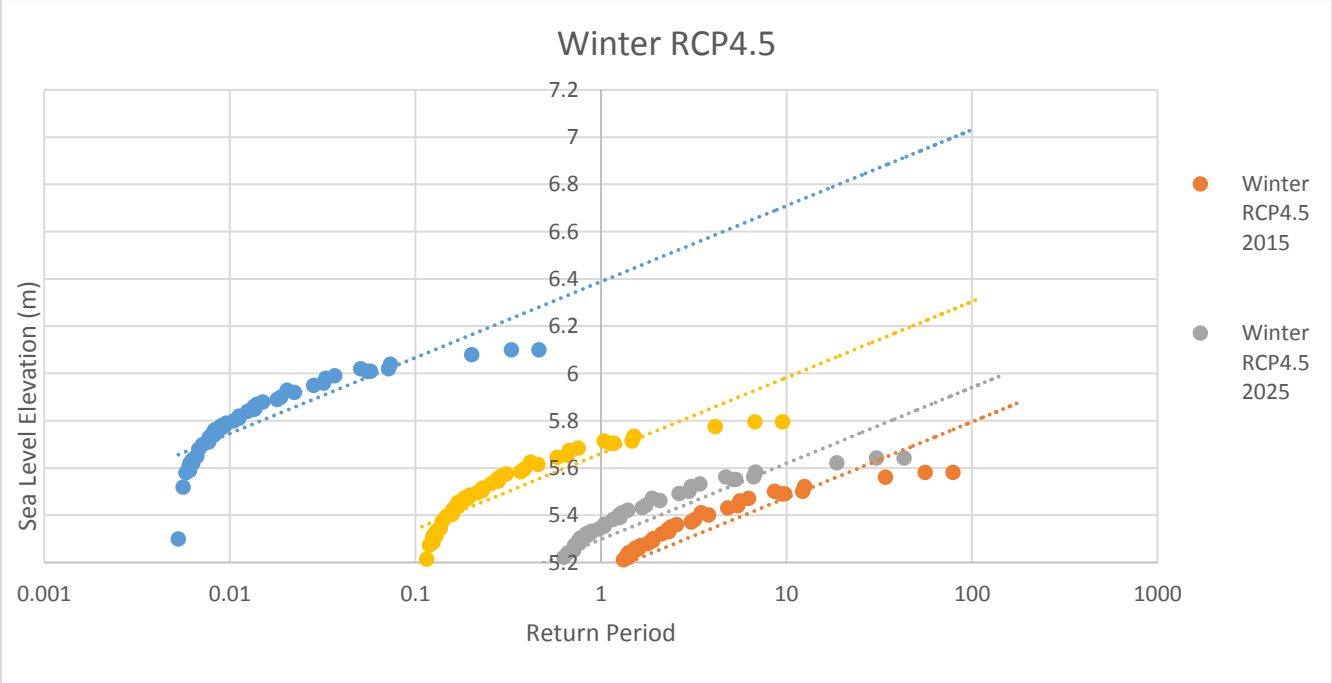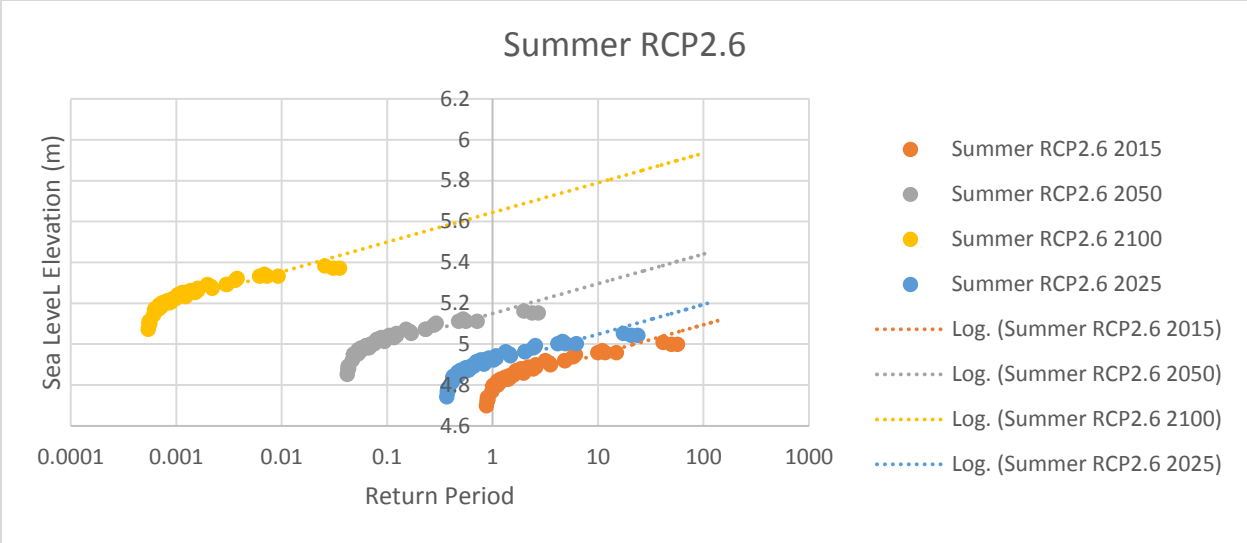
```
% 95% confidence intervals

kCI6 = paramCIs6(:,1)

sigmaCI6 = paramCIs6(:,2)

muCI6 = paramCIs6(:,3)
```
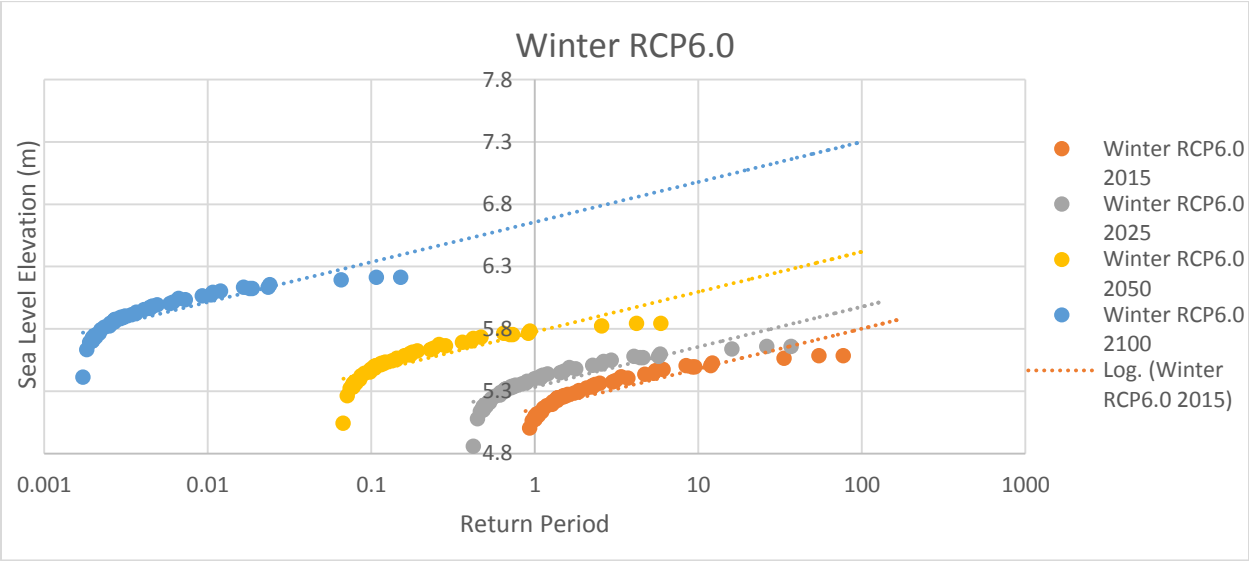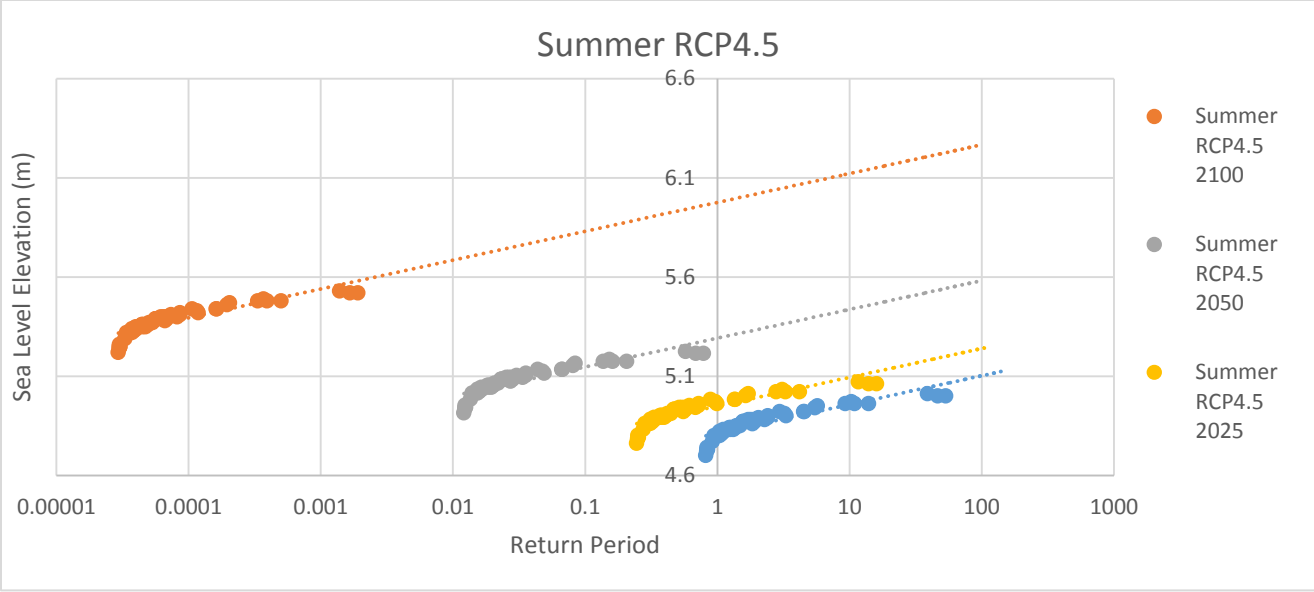
Appendix F: CDF graphs

Summer RCP2.6

Winter RCP4.5

Summer RCP4.5

Winter RCP6.0

Summer RCP8.5
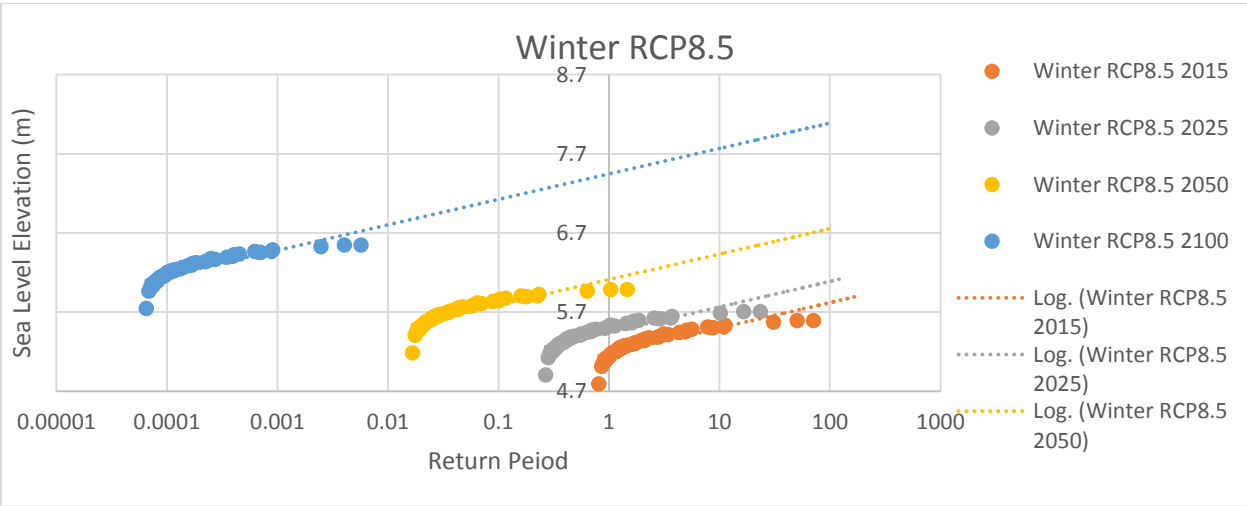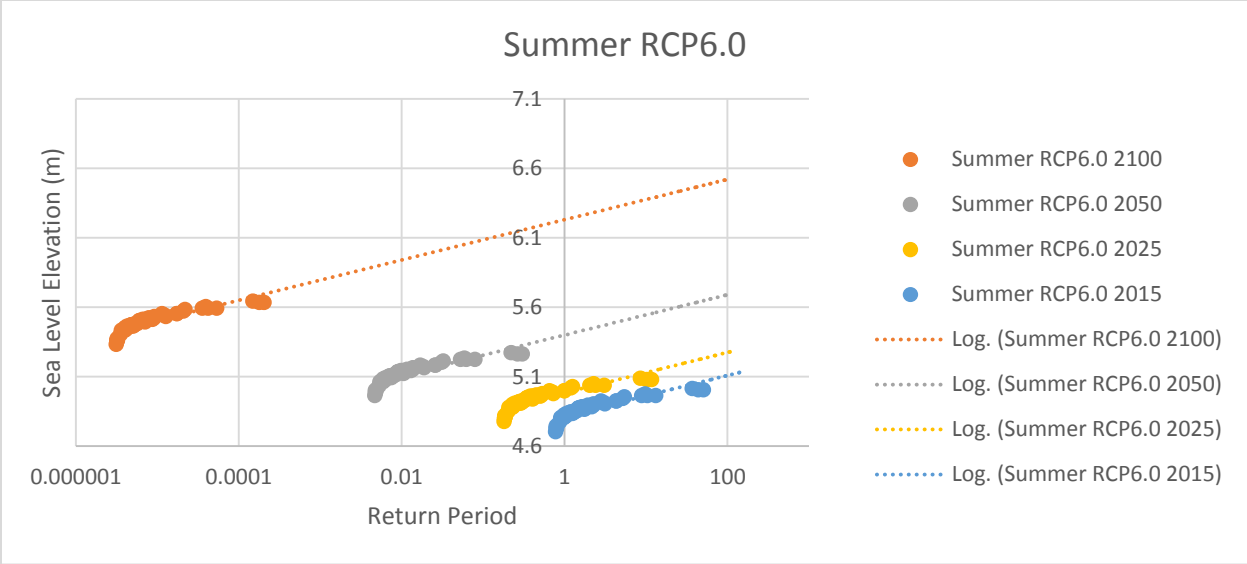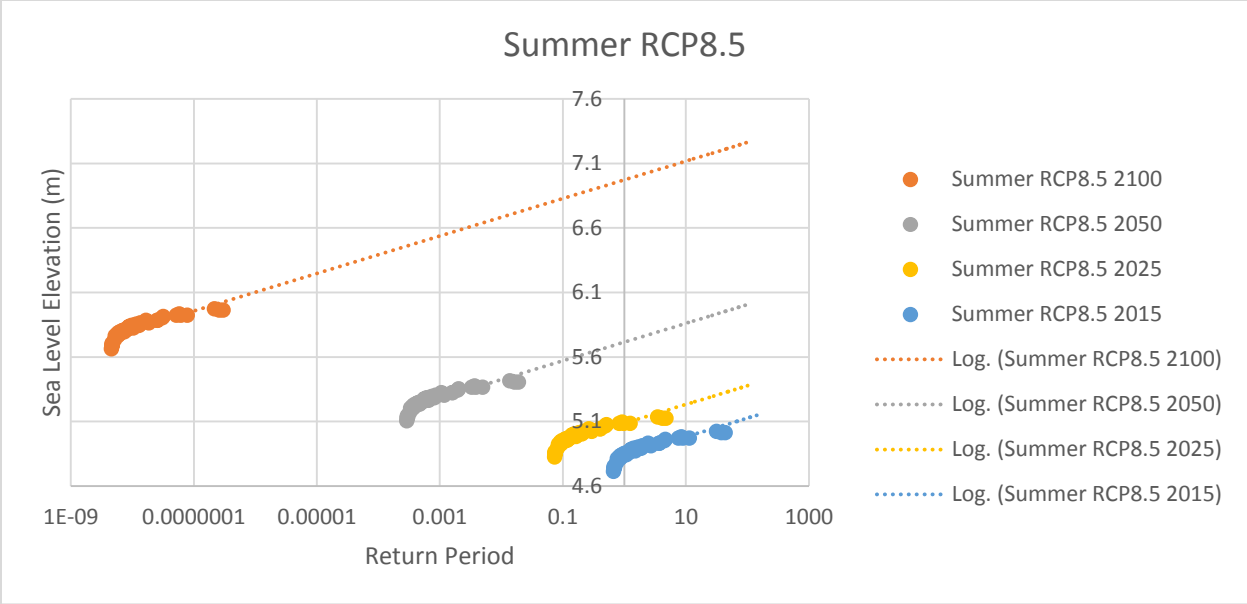
Appendix G: Probabilistic method details

Season	Scenario	Timescale	Logothrimic Equation	Return Periods	Sea Level	Corrected to Geodetic Datum
Winter	RCP2.6	2015	y = 0.1396ln(x) + 5.1444	10	5.465840879	2.855840879
				25	5.593755065	2.983755065
				50	5.690518412	3.080518412
				100	5.787281758	3.177281758
				200	5.884045104	3.274045104
		2025	y = 0.1396ln(x) + 5.2493	10	5.570740879	2.960740879
				25	5.698655065	3.088655065
				50	5.795418412	3.185418412
				100	5.892181758	3.282181758
				200	5.988945104	3.378945104
		2050	y = 0.1396ln(x) + 5.5114	10	5.832840879	3.222840879
				25	5.960755065	3.350755065
				50	6.057518412	3.447518412
				100	6.154281758	3.544281758
				200	6.251045104	3.641045104
		2100	y = 0.1396ln(x) + 6.0357	10	6.357140879	3.747140879
				25	6.485055065	3.875055065
				50	6.581818412	3.971818412
				100	6.678581758	4.068581758
				200	6.775345104	4.165345104
Summer	RCP2.6	2015	y= 0.063ln(x) + 4.8045	10	4.949562861	2.339562861
				25	5.007289177	2.397289177
				50	5.050957449	2.440957449
				100	5.094625722	2.484625722
				200	5.138293994	2.528293994
		2025	y = 0.063ln(x) + 4.9033	10	5.048362861	2.438362861
				25	5.106089177	2.496089177
				50	5.149757449	2.539757449
				100	5.193425722	2.583425722
				200	5.237093994	2.627093994
		2050	y = 0.063ln(x) + 5.1502	10	5.295262861	2.685262861
				25	5.352989177	2.742989177
				50	5.396657449	2.786657449
				100	5.440325722	2.830325722
				200	5.483993994	2.873993994
		2100	y = 0.063ln(x) + 5.6441	10	5.789162861	3.179162861
				25	5.846889177	3.236889177
				50	5.890557449	3.280557449
				100	5.934225722	3.324225722
				200	5.977893994	3.367893994

Season	Scenario	Timescale	Logothrimic Equation	Return Periods	Sea Level	Corrected to Geodetic Datum
Winter	RCP6.0	2015	y = 0.1396ln(x) + 5.1587	10	5.480140879	2.870140879
				25	5.608055065	2.998055065
				50	5.704818412	3.094818412
				100	5.801581758	3.191581758
				200	5.898345104	3.288345104
		2025	y = 0.1396ln(x) + 5.3351	10	5.656540879	3.046540879
				25	5.784455065	3.174455065
				50	5.881218412	3.271218412
				100	5.977981758	3.367981758
				200	6.074745104	3.464745104
		2050	y = 0.1396ln(x) + 5.776	10	6.097440879	3.487440879
				25	6.225355065	3.615355065
				50	6.322118412	3.712118412
				100	6.418881758	3.808881758
				200	6.515645104	3.905645104
		2100	y = 0.1396ln(x) + 6.6577	10	6.979140879	4.369140879
				25	7.107055065	4.497055065
				50	7.203818412	4.593818412
				100	7.300581758	4.690581758
				200	7.397345104	4.787345104
Summer	RCP6.0	2015	y = 0.063ln(x) + 4.818	10	4.963062861	2.353062861
				25	5.020789177	2.410789177
				50	5.064457449	2.454457449
				100	5.108125722	2.498125722
				200	5.151793994	2.541793994
		2025	y = 0.063ln(x) + 4.9841	10	5.129162861	2.519162861
				25	5.186889177	2.576889177
				50	5.230557449	2.620557449
				100	5.274225722	2.664225722
				200	5.317893994	2.707893994
		2050	y = 0.063ln(x) + 5.3994	10	5.544462861	2.934462861
				25	5.602189177	2.992189177
				50	5.645857449	3.035857449
				100	5.689525722	3.079525722
				200	5.733193994	3.123193994
		2100	y = 0.063ln(x) + 6.23	10	6.375062861	3.765062861
				25	6.432789177	3.822789177
				50	6.476457449	3.866457449
				100	6.520125722	3.910125722
				200	6.563793994	3.953793994

Season	Scenario	Timescale	Logothrimic Equation	Return Periods	Sea Level	Corrected to Geodetic Datum
Winter	RCP8.5	2015	y = 0.1396ln(x) + 5.1768	10	5.498240879	2.888240879
				25	5.626155065	3.016155065
				50	5.722918412	3.112918412
				100	5.819681758	3.209681758
				200	5.916445104	3.306445104
		2025	y = 0.1396ln(x) + 5.4438	10	5.765240879	3.155240879
				25	5.893155065	3.283155065
				50	5.989918412	3.379918412
				100	6.086681758	3.476681758
				200	6.183445104	3.573445104
		2050	y = 0.1396ln(x) + 6.111	10	6.432440879	3.822440879
				25	6.560355065	3.950355065
				50	6.657118412	4.047118412
				100	6.753881758	4.143881758
				200	6.850645104	4.240645104
		2100	y = 0.1396ln(x) + 7.4456	10	7.767040879	5.157040879
				25	7.894955065	5.284955065
				50	7.991718412	5.381718412
				100	8.088481758	5.478481758
				200	8.185245104	5.575245104
Summer	RCP8.5	2015	y = 0.063ln(x) + 4.835	10	4.980062861	2.370062861
				25	5.037789177	2.427789177
				50	5.081457449	2.471457449
				100	5.125125722	2.515125722
				200	5.168793994	2.558793994
		2025	y = 0.063ln(x) + 5.0865	10	5.231562861	2.621562861
				25	5.289289177	2.679289177
				50	5.332957449	2.722957449
				100	5.376625722	2.766625722
				200	5.420293994	2.810293994
		2050	y = 0.063ln(x) + 5.7151	10	5.860162861	3.250162861
				25	5.917889177	3.307889177
				50	5.961557449	3.351557449
				100	6.005225722	3.395225722
				200	6.048893994	3.438893994
		2100	y = 0.063ln(x) + 6.9722	10	7.117262861	4.507262861
				25	7.174989177	4.564989177
				50	7.218657449	4.608657449
				100	7.262325722	4.652325722
				200	7.305993994	4.695993994

Season	Scenario	Timescale	Logothrimic Equation	Return Periods	Sea Level	Correct to Geodetic Datum
Winter	RCP4.5	2015	y = 0.1396ln(x) + 5.1525	10	5.473940879	2.863940879
				25	5.601855065	2.991855065
				50	5.698618412	3.088618412
				100	5.795381758	3.185381758
				200	5.892145104	3.282145104
		2025	y = 0.1396ln(x) + 5.2979	10	5.619340879	3.009340879
				25	5.747255065	3.137255065
				50	5.844018412	3.234018412
				100	5.940781758	3.330781758
				200	6.037545104	3.427545104
		2050	y = 0.1396ln(x) + 5.6613	10	5.982740879	3.372740879
				25	6.110655065	3.500655065
				50	6.207418412	3.597418412
				100	6.304181758	3.694181758
				200	6.400945104	3.790945104
		2100	y = 0.1396ln(x) + 6.3882	10	6.709640879	4.099640879
				25	6.837555065	4.227555065
				50	6.934318412	4.324318412
				100	7.031081758	4.421081758
				200	7.127845104	4.517845104
Summer	RCP4.5	2015	y = 0.063ln(x) + 4.8121	10	4.957162861	2.347162861
				25	5.014889177	2.404889177
				50	5.058557449	2.448557449
				100	5.102225722	2.492225722
				200	5.145893994	2.535893994
		2025	y = 0.063ln(x) + 4.9491	10	5.094162861	2.484162861
				25	5.151889177	2.541889177
				50	5.195557449	2.585557449
				100	5.239225722	2.629225722
				200	5.282893994	2.672893994
		2050	y = 0.063ln(x) + 5.2914	10	5.436462861	2.826462861
				25	5.494189177	2.884189177
				50	5.537857449	2.927857449
				100	5.581525722	2.971525722
				200	5.625193994	3.015193994
		2100	y = 0.063ln(x) + 5.9761	10	6.121162861	3.511162861
				25	6.178889177	3.568889177
				50	6.222557449	3.612557449
				100	6.266225722	3.656225722
				200	6.309893994	3.699893994

Appendix H: Separation value details

Separation Values for Vancouver					
Station Number	Station Name	Latitude	Longitude	Separation Value	Considered
7625	MIDDLE ARM	49.19	123.14	2.25	Yes
7634	NORTH ARM	49.23	123.25	2.7	Yes
7635	POINT GREY	49.25	123.27	2.9	Yes
7640	NORTH ARM AT FRASER ST	49.21	123.09	2	Yes
7654	NEW WESTMINSTER	49.2	122.91	1.3	Yes
7710	FALSE CREEK			3.02	No
7735	VANCOUVER	49.29	123.11	3	Yes
7743	ALBERTA POOL ELEVATORS	49.29	123.03	3.18	Yes
7747	STANOVAN	49.29	123.01	3.02	Yes
7755	PORT MOODY	49.29	122.87	3.14	Yes
7765	DEEP COVE	49.33	122.95	3.07	No
7786	Sandy Cove; W Vancouver ,			3.07	No
7795	POINT ATKINSON	49.34	123.25	3.06	No
	Average			2.61	

RCP 2.6 2014

RCP 2.6 2050

RCP 2.6 2100

RCP 8.5 2014
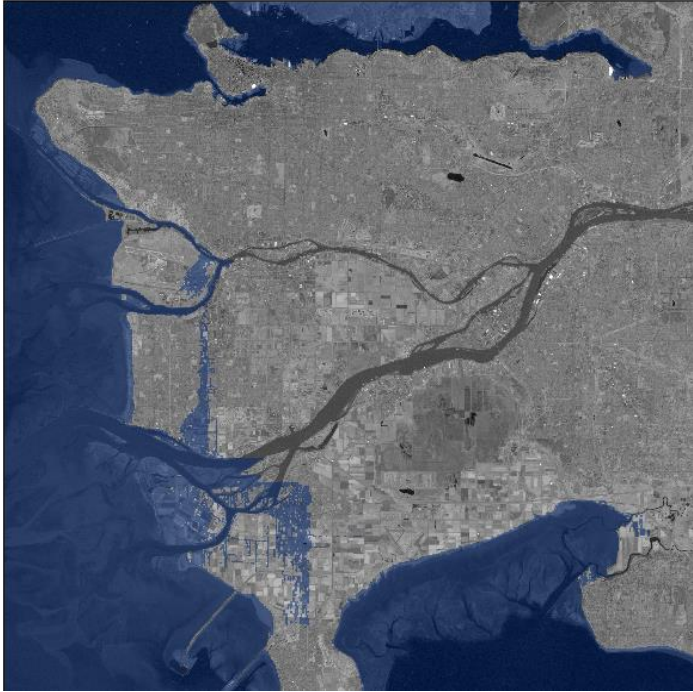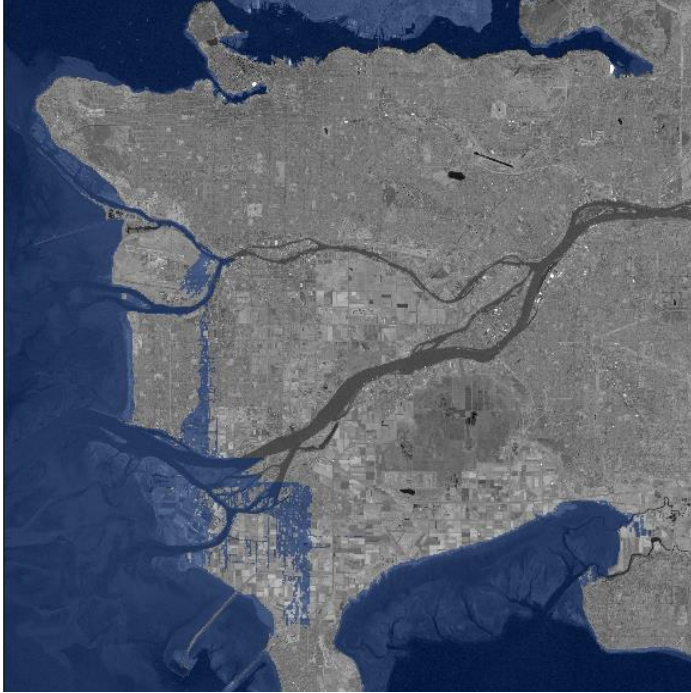
RCP 8.5 2050

RCP 8.5 2100

Appendix J: Method 2 results: Probabilistic analysis

Summer RCP 2.6 2025 200
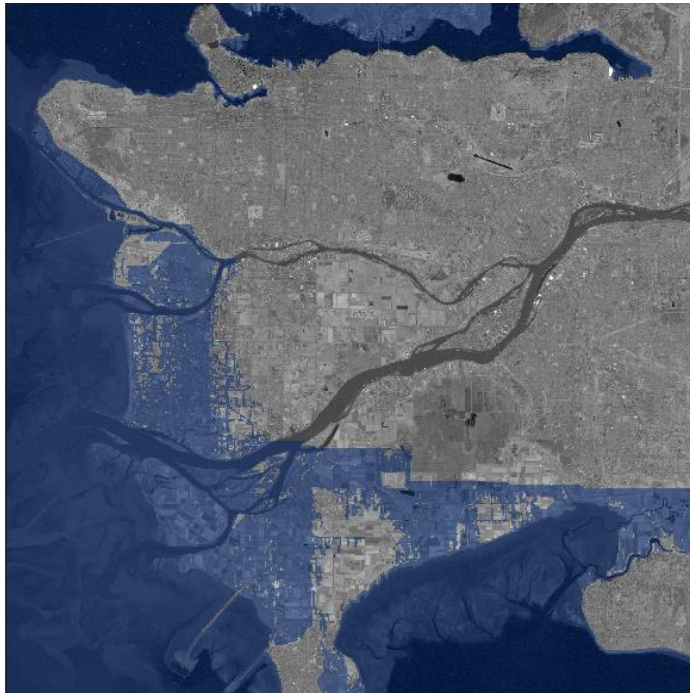

Summer RCP 2.6 2100 200

Summer RCP 8.5 2025 200

Summer RCP 8.5 2100 200

Winter RCP 2.6 2025 200

Winter RCP 2.6 2100 200

Winter RCP 8.5 2025 200

Winter RCP 8.5 2100 200

Appendix K: List of Previous Reports in the Series

ISSN: (Print) 1913-3200; (online) 1913-3219

In addition to 70 previous reports (No. 01 – No. 70) prior to 2011

Tarana A. Solaiman and Slobodan P. Simonovic (2011). Quantifying Uncertainties in the Modelled Estimates of Extreme Precipitation Events at Upper Thames River Basin. Water Resources Research Report no. 070, Facility for Intelligent Decision Support, Department of Civil and Environmental Engineering, London, Ontario, Canada, 167 pages. ISBN: (print) 978-0-7714-2878-4; (online) 978-0-7714-2880-7.

Tarana A. Solaiman and Slobodan P. Simonovic (2011). Assessment of Global and Regional Reanalyses Data for Hydro-Climatic Impact Studies in the Upper Thames River Basin. Water Resources Research Report no. 071, Facility for Intelligent Decision Support, Department of Civil and Environmental Engineering, London, Ontario, Canada, 74 pages. ISBN: (print) 978-0-7714-2892-0; (online) 978-0-7714-2899-9.

Tarana A. Solaiman and Slobodan P. Simonovic (2011). Development of Probability Based Intensity-Duration-Frequency Curves under Climate Change. Water Resources Research Report no. 072, Facility for Intelligent Decision Support, Department of Civil and Environmental Engineering, London, Ontario, Canada, 89 pages. ISBN: (print) 978-0-7714-2893-7; (online) 978-0-7714-2900-2.

Dejan Vucetic and Slobodan P. Simonovic (2011). Water Resources Decision Making Under Uncertainty. Water Resources Research Report no. 073, Facility for Intelligent Decision Support, Department of Civil and Environmental Engineering, London, Ontario, Canada, 143 pages. ISBN: (print) 978-0-7714-2894-4; (online) 978-0-7714-2901-9.

Angela Peck, Elisabeth Bowering, and Slobodan P. Simonovic (2011). City of London: Vulnerability of Infrastructure to Climate Change, Final Report. Water Resources Research Report no. 074, Facility for Intelligent Decision Support, Department of Civil and Environmental

Engineering, London, Ontario, Canada, 66 pages. ISBN: (print) 978-0-7714-2895-1; (online) 978-0-7714-2902-6.

M. Khaled Akhtar, Slobodan P. Simonovic, Jacob Wibe, Jim MacGee and Jim Davies (2011). An Integrated System Dynamics Model for Analyzing Behaviour of the Social-Energy-Economy-Climate System: Model Description. Water Resources Research Report no. 075, Facility for Intelligent Decision Support, Department of Civil and Environmental Engineering, London, Ontario, Canada, 211 pages. ISBN: (print) 978-0-7714-2896-8; (online) 978-0-7714-2903-3.

M. Khaled Akhtar, Slobodan P. Simonovic, Jacob Wibe, Jim MacGee and Jim Davies (2011). An Integrated System Dynamics Model for Analyzing Behaviour of the Social-Energy-Economy-Climate System: User's Manual. Water Resources Research Report no. 076, Facility for Intelligent Decision Support, Department of Civil and Environmental Engineering, London, Ontario, Canada, 161 pages. ISBN: (print) 978-0-7714-2897-5; (online) 978-0-7714-2904-0.

Nick Millington, Samiran Das and Slobodan P. Simonovic (2011). The Comparison of GEV, Log-Pearson Type 3 and Gumbel Distributions in the Upper Thames River Watershed under Global Climate Models. Water Resources Research Report no. 077, Facility for Intelligent Decision Support, Department of Civil and Environmental Engineering, London, Ontario, Canada, 53 pages. ISBN: (print) 978-0-7714-2898-2; (online) 978-0-7714-2905-7.

Andre Schardong and Slobodan P. Simonovic (2011). Multi-objective Evolutionary Algorithms for Water Resources Management. Water Resources Research Report no. 078, Facility for Intelligent Decision Support, Department of Civil and Environmental Engineering, London, Ontario, Canada, 167 pages. ISBN: (print) 978-0-7714-2907-1; (online) 978-0-7714-2908-8.

Samiran Das and Slobodan P. Simonovic (2012). Assessment of Uncertainty in Flood Flows under Climate Change. Water Resources Research Report no. 079, Facility for Intelligent Decision Support, Department of Civil and Environmental Engineering, London, Ontario, Canada, 67 pages. ISBN: (print) 978-0-7714-2960-6; (online) 978-0-7714-2961-3.

Rubaiya Sarwar, Sarah E. Irwin, Leanna King and Slobodan P. Simonovic (2012). Assessment of Climatic Vulnerability in the Upper Thames River basin: Downscaling with SDSM. Water Resources Research Report no. 080, Facility for Intelligent Decision Support, Department of Civil and Environmental Engineering, London, Ontario, Canada, 65 pages. ISBN: (print) 978-0-7714-2962-0; (online) 978-0-7714-2963-7.

Sarah E. Irwin, Rubaiya Sarwar, Leanna King and Slobodan P. Simonovic (2012). Assessment of Climatic Vulnerability in the Upper Thames River basin: Downscaling with LARS-WG. Water Resources Research Report no. 081, Facility for Intelligent Decision Support, Department of Civil and Environmental Engineering, London, Ontario, Canada, 80 pages. ISBN: (print) 978-0-7714-2964-4; (online) 978-0-7714-2965-1.

Samiran Das and Slobodan P. Simonovic (2012). Guidelines for Flood Frequency Estimation under Climate Change. Water Resources Research Report no. 082, Facility for Intelligent Decision Support, Department of Civil and Environmental Engineering, London, Ontario, Canada, 44 pages. ISBN: (print) 978-0-7714-2973-6; (online) 978-0-7714-2974-3.

Angela Peck and Slobodan P. Simonovic (2013). Coastal Cities at Risk (CCaR): Generic System Dynamics Simulation Models for Use with City Resilience Simulator. Water Resources Research Report no. 083, Facility for Intelligent Decision Support, Department of Civil and Environmental Engineering, London, Ontario, Canada, 55 pages. ISBN: (print) 978-0-7714-3024-4; (online) 978-0-7714-3025-1.

Roshan Srivastav and Slobodan P. Simonovic (2014). Generic Framework for Computation of Spatial Dynamic Resilience. Water Resources Research Report no. 085, Facility for Intelligent Decision Support, Department of Civil and Environmental Engineering, London, Ontario, Canada, 81 pages. ISBN: (print) 978-0-7714-3067-1; (online) 978-0-7714-3068-8.

Angela Peck and Slobodan P. Simonovic (2014). Coupling System Dynamics with Geographic Information Systems: CCaR Project Report. Water Resources Research Report no. 086, Facility

for Intelligent Decision Support, Department of Civil and Environmental Engineering, London, Ontario, Canada, 60 pages. ISBN: (print) 978-0-7714-3069-5; (online) 978-0-7714-3070-1.

Sarah Irwin, Roshan Srivastav and Slobodan P. Simonovic (2014). Instruction for Watershed Delineation in an ArcGIS Environment for Regionalization Studies.Water Resources Research Report no. 087, Facility for Intelligent Decision Support, Department of Civil and Environmental Engineering, London, Ontario, Canada, 45 pages. ISBN: (print) 978-0-7714-3071-8; (online) 978-0-7714-3072-5.

Andre Schardong, Roshan K. Srivastav and Slobodan P. Simonovic (2014).Computerized Tool for the Development of Intensity-Duration-Frequency Curves under a Changing Climate: Users Manual v.1 Water Resources Research Report no. 088, Facility for Intelligent Decision Support, Department of Civil and Environmental Engineering, London, Ontario, Canada, 68 pages. ISBN: (print) 978-0-7714-3085-5; (online) 978-0-7714-3086-2.

Roshan K. Srivastav, Andre Schardong and Slobodan P. Simonovic (2014). Computerized Tool for the Development of Intensity-Duration-Frequency Curves under a Changing Climate: Technical Manual v.1 Water Resources Research Report no. 089, Facility for Intelligent Decision Support, Department of Civil and Environmental Engineering, London, Ontario, Canada, 62 pages. ISBN: (print) 978-0-7714-3087-9; (online) 978-0-7714-3088-6.

Roshan K. Srivastav and Slobodan P. Simonovic (2014). Simulation of Dynamic Resilience: A Railway Case Study. Water Resources Research Report no. 090, Facility for Intelligent Decision Support, Department of Civil and Environmental Engineering, London, Ontario, Canada, 91 pages. ISBN: (print) 978-0-7714-3089-3; (online) 978-0-7714-3090-9.